Bending, buckling and free vibration behaviours of thin-walled functionally graded sandwich and composite channel-section beams

Ngoc-Duong Nguyen[a], Trung-Kien Nguyen[a,*], Thuc P. Vo[b], Lieu B. Nguyen[a]

[a] Faculty of Civil Engineering, Ho Chi Minh City University of Technology and Education, 1 Vo Van Ngan Street, Thu Duc District, Ho Chi Minh City, Viet Nam.

[b] School of Engineering and Mathematical Sciences, La Trobe University, Bundoora, VIC 3086, Australia.

Abstract

This paper proposes static, free vibration and buckling analysis of thin-walled functionally graded sandwich and composite channel-section beams. It is based on the first-order shear deformable beam theory, which can recover to classical one by ignoring the shear effect. Ritz's approximation functions are developed to solve the characteristic problems. Both results from classical and the first-order shear deformable theories are given in a unified fashion. Ritz solutions are applied for thin-walled FG sandwich channel-section beams for the first time. Numerical examples are presented in relation to many important effects such as span-to-height ratio, material parameter, lay-ups, fiber orientation and boundary conditions on the beams' deflections, natural frequencies and critical buckling loads. New results presented in this study can be of interests to the scientific and engineering community in the future.

Keywords: Ritz solutions; Thin-walled beams; Laminated composite and FG channel beams; bending, buckling and vibration behaviours.

* Corresponding author.

E-mail address: kiennt@hcmute.edu.vn (Trung-Kien Nguyen)

1. Introduction

Functionally graded (FG) and composite materials are widely used in many engineering fields owing to their high strength-to-weight and stiffness-to-weight ratio, long-term durability and non-corrosive nature. Most recent applications in civil, transportation and mechanical industries show the effectiveness of thin-walled FG and composite structures (Dechao, Zhongmin and Xingwei 2001; Librescu and Song 2005; Pawar and Ganguli 2006; Moon et al. 2010; Arnaud et al. 2011; Alizada, Sofiyev and Kuruoglu 2012; Harursampath, Harish and Hodges 2017b; Xu, Zhang and Zhang 2018; Sofiyev 2019). They also attracted a large number of researchers to study the structural responses, in which, vibration, bending and buckling behaviours are the importance and interest to the performance.

Thin-walled beam theory was firstly introduced for isotropic material by Vlasov, which was also called Vlasov's classical beam theory (Vlasov 1961). It was then extended to composite material by many authors and some of them were mentioned here. Bauld and Lih-Shyng (1984) developed Vlasov's theory for bending and buckling analysis of thin-walled composite beams. Kim, Shin and Kim (2006) analysed thin-walled composite channel and I-beams under torsion. Bending behaviours of composite I-beams were presented by Shin, Kim and Kim (2007). Nguyen, Kim and Lee (2016a) and Nguyen, Kim and Lee (2016b) predicted the deflections and vibration of thin-walled FG sandwich beams with channel and I-sections. Vo and Lee (2013) proposed a finite element method for vibration and buckling analysis of thin-walled composite I-beams with arbitrary lay-ups under axial loads and end moments. Kim and Lee (2015) developed refined theory for analysing thin-walled composite beams on elastic foundations. Recently, Kim and Lee (2017a) analysed bending responses of thin-walled

FG sandwich beams under torsion and vertical load. Zhu et al. (2016), Malekshahi, Hosseini and Ansari (2020) proposed theoretical estimation for vibration and post buckling structure with hollow sections. It can be seen that although the classical beam theory is simply but it ignores the shear effect, which becomes significant for the thick beams. Therefore, in order to account this effect, a large number of studies are developed to predict behaviours of thin-walled composite beams. Mao and Lin (1996) studied buckling and post-buckling behaviours of thin-walled composite beams with simply-supported boundary conditions using trigonometric series solutions and perturbation method. Pagani, Carrera and Ferreira (2016) investigated free vibrations of thin-walled beams using higher-order shear deformation theories and radial shape functions. Ascione, Feo and Mancusi (2000) proposed a shear deformable model to determine the deflections of composite channel beams. Lee (2005) analysed bending behaviours of thin-walled composite I-beams. Sheikh and Thomsen (2008) presented a new beam element to analyse thin-walled composite beams with open or closed section. Cortínez and Piovan (2006) analysed nonlinear buckling thin-walled composite beams including shear effects. Back and Will (2008) predicted the buckling loads and deflections of thin-walled composite I-beams. Kim and Lee (2014) proposed exact solution for vibration and buckling of thin-walled composite beams with open section. Maceri and Vairo (2009) proposed a new model for thin-walled anisotropic beams. The shear deformable theory was also used by Kim and Lee (2017b) to analyse thin-walled FG sandwich I-beams. Pavazza, Matoković and Vukasović (2020) proposed a torsion theory for isotropic thin-walled beams considering shear effect. Sofiyev (2014), Sofiyev et al. (2016a), Sofiyev et al. (2016b), and Sofiyev and Osmancelebioglu (2017) analysed buckling and vibration of FG cylindrical shells based on a first order shear deformation theory. In these studies, authors investigated the effects of shear stress, FG core, sandwich shell geometry on critical loads and frequencies of shell. For computational approach, the finite element method (FEM) is increasingly used for bending and buckling analysis of thin-walled composite beams. Kollár and Pluzsik (2012) analysed bending and torsion behaviours of thin-walled composite beams. Aguiar, Moleiro and Soares (2012) developed FEM to analyse bending of composite beams with various cross-sections. Günay and Timarci (2017) presented static behaviours of thin-walled composite beams with closed-section by the classical beam theory. Kim and Lee (2018) proposed a nonlinear model of thin-walled FG I-beams. Kim and Jeon (2013) analysed static and dynamic behaviours of thin-walled composite channel beams by a shear deformable theory. FEM is also used to analyse bending, buckling and vibration of FG beam with honeycomb core (Li, Shen and Wang 2019b; Li, Shen and Wang 2019d; Li, Shen and Wang 2019c; Li, Shen and Wang 2019a). Later, by stiffness matrix method and FEM, Kim, Jeon and Lee (2013), Kim and Shin (2009), and Kim (Kim 2011; Kim 2012) determined the deflections of thin-walled composite beams with mono-symmetric I-, L- and channel section. Lanc et al. (2016) used FEM to analyse buckling behaviours of thin-walled FG beams. Isogeometric analysis method was used to deal with thin-walled composite curved beams (Cárdenas et al. 2018). Harursampath, Harish and Hodges (2017a) proposed the variational asymptotic method and used Monte-Carlo-type stochastic approach for behaviour analysis of thin-walled composite beams. Ritz method is simple and effective to analyse bending, buckling and free vibration of composite beams with rectangular cross-section (Aydogdu 2006a; Aydogdu 2006b; Şimşek 2009; Pradhan and Chakraverty 2013; Mantari and Canales 2016; Nguyen et al. 2017), however, it is rarely used for thin-walled composite beams.

Qiao and Zou (2002) presented free vibration of fiber-reinforced plastic composite cantilever I-beams using the Ritz method with transcendental and polynomial shape functions satisfying the boundary conditions. Nguyen et al. (2019) developed the Ritz method for vibration and buckling of thin-walled composite I-beams. From literature review, Ritz method has not been previously used to analyse vibration, bending and buckling behaviours of thin-walled composite channel beams. Due to asymmetric geometric and material anisotropic of composite channel section, shear center and centroid are not coincided. This causes coupling responses from axial, bending, lateral, torsional and warping behaviours thus their structural responses are is very complex. Besides, it can be seen that the effect of shear deformation on the structural responses of thin-walled FG sandwich channel-section beams has not been available yet. Therefore, there is a need for further studies related to these complicated problems.

This paper, which is extended from previous study (Nguyen et al. 2019), focuses on bending, vibration and buckling analysis of thin-walled FG sandwich and composite channel beams. It is based on the first-order shear deformation theory, which can recover to classical one by ignoring the shear effect. Lagrange's equations are employed to formulate the governing equations to describe the structural responses of beams and Ritz method is used to solve the problems. Numerical examples are performed to verify accuracy and efficiency of the present solutions. Many significant effects such as span-to-height ratio, material parameter, lay-ups, fiber orientation, boundary conditions on the beams' deflection, frequency and critical buckling load are investigated.

2. Theoretical formulation

In this section, a displacement field and constitutive equations of thin-wall FG sandwich and composite beams are established. Next, their strain energy, work done by external forces and total potential energy are determined, and finally the Ritz method is proposed to solve structural responses of such beams with various boundary conditions.

In order to develop displacement field of thin-walled beams, local coordinate system (n, s, z), Cartesian coordinate system (x, y, z) and contour coordinate S along the profile of the section are used as shown in Fig. 1 (Lee 2001). The P is called the shear center and the axis, which is through P and parallel to the axis z, is called the pole axis. θ is an angle of orientation between (n, s, z) and (x, y, z) coordinate systems. r and q are coordinates of any point on the contour measured from P in (n, s, z) coordinate system. The basic assumptions are (a) the contour of section does not deform in its own plane; (b) shear strains $\gamma_{xz}^0, \gamma_{yz}^0$ and warping shear γ_{ϖ}^0 are uniform over the section; (c) Poisson's coefficient is constant.

2.1. Kinematics

The displacements (u, v, w) at any point in the contour are expressed through the mid-surface displacements ($\bar{u}$, $\bar{v}$, $\bar{w}$) and the rotations of transverse normal about s and z $(\bar{\psi}_s, \bar{\psi}_z)$ as followings (Lee 2005; Vo and Lee 2009; Nguyen et al. 2019):

$$u(n,s,z,t) = \bar{u}(s,z,t) \tag{1a}$$

$$v(n,s,z,t) = \bar{v}(s,z,t) + n\bar{\psi}_s(s,z,t) \tag{1b}$$

$$w(n,s,z,t) = \bar{w}(s,z,t) + n\bar{\psi}_z(s,z,t) \tag{1c}$$

The mid-surface displacements ($\bar{u}$, $\bar{v}$, $\bar{w}$) and rotations of transverse normal about s and z $(\bar{\psi}_s, \bar{\psi}_z)$ are related to displacements of P in x-, y- and z- directions (U, V, W) and rotations of the cross-section with respect to x, y, ϖ and pole axis $(\psi_x, \psi_y, \psi_\varpi, \phi)$ as (Lee 2005; Vo and Lee 2009; Kim and Lee 2017b; Nguyen et al. 2019):

$$\bar{u}(s,z,t) = U(z,t)\sin\theta(s) - V(z,t)\cos\theta(s) - \phi(z,t)q(s) \tag{2a}$$

$$\bar{v}(s,z,t) = U(z,t)\cos\theta(s) + V(z,t)\sin\theta(s) + \phi(z,t)r(s) \tag{2b}$$

$$\bar{w}(s,z,t) = W(z,t) + \psi_y(z,t)x(s) + \psi_x(z,t)y(s) + \psi_\varpi(z,t)\varpi(s) \tag{2c}$$

$$\bar{\psi}_z = \psi_y \sin\theta - \psi_x \cos\theta - \psi_\varpi q \tag{2d}$$

$$\bar{\psi}_s(s,z) = -\frac{\partial \bar{u}}{\partial s} \tag{2e}$$

where

$$\psi_y = \gamma_{xz}^0 - U' \tag{3a}$$

$$\psi_x = \gamma_{yz}^0 - V' \tag{3b}$$

$$\psi_\varpi = \gamma_\varpi^0 - \phi' \tag{3c}$$

and the prime designates the derivative with respect to z; ϖ is warping function given by:

$$\varpi(s) = \int_{s_0}^{s} r(s)ds \tag{4}$$

The non-zero strains of thin-walled beams are defined as (Lee 2005):

$$\varepsilon_z(n,s,z,t) = \bar{\varepsilon}_z(s,z,t) + n\bar{\kappa}_z(s,z,t) = \varepsilon_z^0 + (x + n\sin\theta)\kappa_y + (y - n\cos\theta)\kappa_x + (\varpi - nq)\kappa_\varpi \tag{5a}$$

$$\gamma_{sz}(n,s,z,t) = \bar{\gamma}_{sz}(s,z,t) + n\bar{\kappa}_{sz}(s,z,t) = \gamma_{xz}^0\cos\theta + \gamma_{yz}^0\sin\theta + \gamma_\varpi^0 r + n\kappa_{sz} \tag{5b}$$

$$\gamma_{nz}(n,s,z,t) = \bar{\gamma}_{nz}(s,z,t) + n\bar{\kappa}_{nz}(s,z,t) = \gamma_{xz}^0\sin\theta - \gamma_{yz}^0\cos\theta - \gamma_\varpi^0 q \tag{5c}$$

where

$$\bar{\varepsilon}_z = \frac{\partial \bar{w}}{\partial z} = \varepsilon_z^0 + x\kappa_y + y\kappa_x + \varpi\kappa_\varpi \tag{6a}$$

$$\bar{\kappa}_z = \frac{\partial \bar{\psi}_z}{\partial z} = \kappa_y \sin\theta - \kappa_x\cos\theta - \kappa_\varpi q \tag{6b}$$

$$\bar{\kappa}_{sz} = \kappa_{sz} \tag{6c}$$

$$\bar{\kappa}_{nz} = 0 \tag{6d}$$

$$\varepsilon_z^0 = W' \tag{6e}$$

$$\kappa_x = \psi_x' \tag{6f}$$

$$\kappa_y = \psi_y' \tag{6g}$$

$$\kappa_\varpi = \psi_\varpi' \tag{6h}$$

$$\kappa_{sz} = \phi' - \psi_\varpi \tag{6i}$$

It can be seen that ε_z^0, κ_x, κ_y, κ_ϖ and κ_{sz} are axial strain, biaxial curvatures in the *x*- and *y*- directions, warping cuvature with respect to the shear center and twisting cuvature in the beam, respectively.

2.2. Constitutive equations

2.2.1. Thin-walled FG sandwich beams

Young's modulus (*E*) and mass density (ρ) of thin-walled FG beams is expressed through the volume fraction of ceramic (V_c), Young's modulus and mass density of ceramic and metal $(E_c, E_m, \rho_c, \rho_m)$:

$$E = E_c V_c + E_m (1 - V_c) \tag{7a}$$

$$\rho = \rho_c V_c + \rho_m (1 - V_c) \tag{7b}$$

Three types of material distributions are considered as follows (Fig. 2):

Type A:

$$V_c = \left[\frac{n}{h} + \frac{1}{2}\right]^p, \quad -0.5h \le n \le 0.5h \tag{8}$$

where h (h_1, h_2, h_3) is the thickness of the flanges or web and p is material parameter.

Type B:

$$V_c = \left[\frac{-|n| + 0.5h}{0.5(1-\alpha)h} \right]^p, \quad -0.5h \le n \le -0.5\alpha h \quad \text{or} \quad 0.5\alpha h \le n \le 0.5h \tag{9a}$$

$$V_c = 1, \quad -0.5\alpha h \le n \le 0.5\alpha h \tag{9b}$$

where $\alpha\ (\alpha_1, \alpha_2, \alpha_3)$ is thickness ratio of ceramic material of the flanges or web.

Type C:

$$V_c = \left[\frac{n + 0.5h}{(1-\alpha)h} \right]^p, \quad -0.5h \le n \le (0.5-\alpha)h \tag{10a}$$

$$V_c = 1, \quad (0.5-\alpha)h \le n \le 0.5h \tag{10b}$$

The stress and strain relations can be written as:

$$\begin{Bmatrix} \sigma_z \\ \sigma_{sz} \\ \sigma_{nz} \end{Bmatrix} = \begin{pmatrix} \bar{Q}_{11}^* & 0 & 0 \\ 0 & \bar{Q}_{66}^* & 0 \\ 0 & 0 & \bar{Q}_{55}^* \end{pmatrix} \begin{Bmatrix} \varepsilon_z \\ \gamma_{sz} \\ \gamma_{nz} \end{Bmatrix} \tag{11}$$

where $$\bar{Q}_{11}^* = E(n), \quad \bar{Q}_{66}^* = \bar{Q}_{55}^* = \frac{E(n)}{2(1+\nu)} \tag{12}$$

and ν is Poisson's coefficient.

2.2.1 Thin-walled composite beams

The stress and strain relations at the k^{th}-layer in (n, s, z) coordinate systems can be determined as:

$$\begin{Bmatrix} \sigma_z \\ \sigma_{sz} \\ \sigma_{nz} \end{Bmatrix}^{(k)} = \begin{pmatrix} \bar{Q}_{11}^* & \bar{Q}_{16}^* & 0 \\ \bar{Q}_{16}^* & \bar{Q}_{66}^* & 0 \\ 0 & 0 & \bar{Q}_{55}^* \end{pmatrix}^{(k)} \begin{Bmatrix} \varepsilon_z \\ \gamma_{sz} \\ \gamma_{nz} \end{Bmatrix} \tag{13}$$

where: $$\bar{Q}_{11}^* = \bar{Q}_{11} - \frac{\bar{Q}_{12}^2}{\bar{Q}_{22}}, \quad \bar{Q}_{16}^* = \bar{Q}_{16} - \frac{\bar{Q}_{12}\bar{Q}_{26}}{\bar{Q}_{22}}, \quad \bar{Q}_{66}^* = \bar{Q}_{66} - \frac{\bar{Q}_{26}^2}{\bar{Q}_{22}}, \quad \bar{Q}_{55}^* = \bar{Q}_{55} \tag{14}$$

In Eq. (14), $\bar{Q}_{ij}$ are the transformed reduced stiffnesses (Reddy 2003).

2.3. Variational formulation

The strain energy Π_E of the system is defined by:

$$\Pi_E = \frac{1}{2}\int_{\Omega}\left(\sigma_z\varepsilon_z + \sigma_{sz}\gamma_{sz} + k^s\sigma_{nz}\gamma_{nz}\right)d\Omega \tag{15}$$

where Ω is volume and k^s is shear correction factor, which is assumed to be a unity in previous study (Nguyen et al. 2019). Substituting Eqs. (5a), (5b), (5c), (11) and (13) into Eq. (15) leads to:

$$\begin{aligned}\Pi_E = \frac{1}{2}\int_0^L \Big[& E_{11}W'^2 + 2E_{16}W'U' + 2E_{17}W'V' + 2\left(E_{15}+E_{18}\right)W'\phi' \\
& +2E_{12}W'\psi_y' + 2E_{16}W'\psi_y + 2E_{13}W'\psi_x' + 2E_{17}W'\psi_x + 2E_{14}W'\psi_\varpi' \\
& +2\left(E_{18}-E_{15}\right)W'\psi_\varpi + E_{66}U'^2 + 2E_{67}U'V' + 2\left(E_{56}+E_{68}\right)U'\phi' + 2E_{26}U'\psi_y' \\
& +2E_{66}U'\psi_y + 2E_{36}U'\psi_x' + 2E_{67}U'\psi_x + 2E_{46}U'\psi_\varpi' + 2\left(E_{68}-E_{56}\right)U'\psi_\varpi + E_{77}V'^2 \\
& +2\left(E_{57}+E_{78}\right)V'\phi' + 2E_{27}V'\psi_y' + 2E_{67}V'\psi_y + 2E_{37}V'\psi_x' + 2E_{77}V'\psi_x + 2E_{47}V'\psi_\varpi' \\
& +2\left(E_{78}-E_{57}\right)V'\psi_\varpi + \left(E_{55}+2E_{58}+E_{88}\right)\phi'^2 + 2\left(E_{25}+E_{28}\right)\phi'\psi_y' + 2\left(E_{56}+E_{68}\right)\phi'\psi_y \\
& +2\left(E_{35}+E_{38}\right)\phi'\psi_x' + 2\left(E_{57}+E_{78}\right)\phi'\psi_x + 2\left(E_{45}+E_{48}\right)\phi'\psi_\varpi' + 2\left(E_{88}-E_{55}\right)\phi'\psi_\varpi \\
& +E_{22}\psi_y'^2 + 2E_{26}\psi_y'\psi_y + E_{66}\psi_y^2 + 2E_{23}\psi_y'\psi_x' + 2E_{27}\psi_y'\psi_x + 2E_{36}\psi_y\psi_x' + 2E_{67}\psi_y\psi_x \\
& +2E_{24}\psi_y'\psi_\varpi' + 2\left(E_{28}-E_{25}\right)\psi_y'\psi_\varpi + 2E_{46}\psi_y\psi_\varpi' + 2\left(E_{68}-E_{56}\right)\psi_y\psi_\varpi + E_{33}\psi_x'^2 \\
& +2E_{37}\psi_x'\psi_x + E_{77}\psi_x^2 + 2E_{34}\psi_x'\psi_\varpi' + 2\left(E_{38}-E_{35}\right)\psi_x'\psi_\varpi + 2E_{47}\psi_x\psi_\varpi' \\
& +2\left(E_{78}-E_{57}\right)\psi_x\psi_\varpi + E_{44}\psi_\varpi'^2 + 2\left(E_{48}-E_{45}\right)\psi_\varpi'\psi_\varpi + \left(E_{88}-2E_{58}+E_{55}\right)\psi_\varpi^2 \Big]dz\end{aligned} \tag{16}$$

where L is length of beam and E_{ij} are the stiffness coefficients of thin-walled FG and composite beam, which depend on the geometry and material distributions in cross-section (see (Lee 2005) for more details).

The work done Π_W of the system by uniform load q_y and concentrated load P_y applied at z_L and axial load N_0 can be expressed as (Lee 2005; Back and Will 2008):

$$\Pi_W = \int_0^L q_y V dz + P_y V\left(z_L\right) + \frac{1}{2}\int_0^L N_0\left(U'^2 + V'^2 + 2y_p U'\phi' - 2x_p V'\phi' + \frac{I_P}{A}\phi'^2\right)dz \tag{17}$$

The kinetic energy Π_K of the system is given by:

$$\Pi_K = \frac{1}{2}\int_\Omega \rho(n)\left(\dot{u}^2 + \dot{v}^2 + \dot{w}^2\right)d\Omega$$

$$= \frac{1}{2}\int_0^L \Big[m_0\dot{W}^2 + 2m_s\dot{W}\dot{\psi}_y - 2m_c\dot{W}\dot{\psi}_x + 2\left(m_\varpi - m_q\right)\dot{W}\dot{\psi}_\varpi + m_0\dot{U}^2 + 2\left(m_c + m_0 y_P\right)\dot{U}\dot{\phi}$$
$$+ m_0\dot{V}^2 + 2\left(m_s - m_0 x_p\right)\dot{V}\dot{\phi} + \left(m_p + m_2 + 2m_r\right)\dot{\phi}^2 + \left(m_{x2} + 2m_{xs} + m_{s2}\right)\dot{\psi}_y^2 \quad (18)$$
$$+2\left(m_{xycs} - m_{cs}\right)\dot{\psi}_y\dot{\psi}_x + 2\left(m_{x\varpi} + m_{x\varpi qs} - m_{qs}\right)\dot{\psi}_y\dot{\psi}_\varpi + \left(m_{y2} - 2m_{yc} + m_{c2}\right)\dot{\psi}_x^2$$
$$+2\left(m_{y\varpi} - m_{y\varpi qc} + m_{qc}\right)\dot{\psi}_x\dot{\psi}_\varpi + \left(m_{\varpi 2} - 2m_{q\varpi} + m_{q2}\right)\dot{\psi}_\varpi^2 \Big] dz$$

where dot-superscript denotes the differentiation with respect to the time t, and the inertia coefficients are defined in Vo and Lee (2009).

The total potential energy of the system is obtained by:

$$\Pi = \Pi_E - \Pi_K - \Pi_W \quad (19)$$

2.4. Ritz solutions

The displacement fields of the thin-walled composite beams are approximated by using Ritz's approximation functions:

$$W(z,t) = \sum_{j=1}^{m} \varphi_j^{'}(z) W_j e^{i\omega t} \quad (20a)$$

$$U(z,t) = \sum_{j=1}^{m} \varphi_j(z) U_j e^{i\omega t} \quad (20b)$$

$$V(z,t) = \sum_{j=1}^{m} \varphi_j(z) V_j e^{i\omega t} \quad (20c)$$

$$\phi(z,t) = \sum_{j=1}^{m} \varphi_j(z) \phi_j e^{i\omega t} \quad (20d)$$

$$\psi_y(z,t) = \sum_{j=1}^{m} \varphi_j^{'}(z) \psi_{yj} e^{i\omega t} \quad (20e)$$

$$\psi_x(z,t) = \sum_{j=1}^{m} \varphi_j^{'}(z)\psi_{xj} e^{i\omega t} \tag{20f}$$

$$\psi_{\varpi}(z,t) = \sum_{j=1}^{m} \varphi_j^{'}(z)\psi_{\varpi j} e^{i\omega t} \tag{20g}$$

where $i^2 = -1$ is the imaginary unit; ω is the frequency; W_j, U_j, V_j, ϕ_j, ψ_{yj}, ψ_{xj} and $\psi_{\varpi j}$ are Ritz's parameters, which need to be determined and $\varphi_j(z)$ are Ritz's approximation functions which depend on boundary conditions (BCs) as seen in Table 1. Four typical BCs as simply-supported (S-S), clamped-free (C-F), clamped-simply supported (C-S) and clamped-clamped (C-C) are considered.

By substituting Eq. (20) into Eq. (19), Lagrange's equations are used to formulate the governing equations:

$$\frac{\partial \Pi}{\partial p_j} - \frac{d}{dt}\frac{\partial \Pi}{\partial \dot{p}_j} = 0 \tag{21}$$

with p_j representing the values of $\left(W_j, U_j, V_j, \phi_j, \psi_{yj}, \psi_{xj}, \psi_{\varpi j}\right)$.

Bending, vibration and buckling behaviours of the thin-walled beams can be obtained by solving the following equation, which presents relations of stiffness matrix $\mathbf{K}$, mass matrix **M,** displacement and force vetor **F**:

$$\left(\begin{bmatrix} \mathbf{K}^{11} & \mathbf{K}^{12} & \mathbf{K}^{13} & \mathbf{K}^{14} & \mathbf{K}^{15} & \mathbf{K}^{16} & \mathbf{K}^{17} \\ {}^{T}\mathbf{K}^{12} & \mathbf{K}^{22} & \mathbf{K}^{23} & \mathbf{K}^{24} & \mathbf{K}^{25} & \mathbf{K}^{26} & \mathbf{K}^{27} \\ {}^{T}\mathbf{K}^{13} & {}^{T}\mathbf{K}^{23} & \mathbf{K}^{33} & \mathbf{K}^{34} & \mathbf{K}^{35} & \mathbf{K}^{36} & \mathbf{K}^{37} \\ {}^{T}\mathbf{K}^{14} & {}^{T}\mathbf{K}^{24} & {}^{T}\mathbf{K}^{34} & \mathbf{K}^{44} & \mathbf{K}^{45} & \mathbf{K}^{46} & \mathbf{K}^{47} \\ {}^{T}\mathbf{K}^{15} & {}^{T}\mathbf{K}^{25} & {}^{T}\mathbf{K}^{35} & {}^{T}\mathbf{K}^{45} & \mathbf{K}^{55} & \mathbf{K}^{56} & \mathbf{K}^{57} \\ {}^{T}\mathbf{K}^{16} & {}^{T}\mathbf{K}^{26} & {}^{T}\mathbf{K}^{36} & {}^{T}\mathbf{K}^{46} & {}^{T}\mathbf{K}^{56} & \mathbf{K}^{66} & \mathbf{K}^{67} \\ {}^{T}\mathbf{K}^{17} & {}^{T}\mathbf{K}^{27} & {}^{T}\mathbf{K}^{37} & {}^{T}\mathbf{K}^{47} & {}^{T}\mathbf{K}^{57} & {}^{T}\mathbf{K}^{67} & \mathbf{K}^{77} \end{bmatrix} - \omega^2 \begin{bmatrix} \mathbf{M}^{11} & \mathbf{0} & \mathbf{0} & \mathbf{0} & \mathbf{M}^{15} & \mathbf{M}^{16} & \mathbf{M}^{17} \\ \mathbf{0} & \mathbf{M}^{22} & \mathbf{0} & \mathbf{M}^{24} & \mathbf{0} & \mathbf{0} & \mathbf{0} \\ \mathbf{0} & \mathbf{0} & \mathbf{M}^{33} & \mathbf{M}^{34} & \mathbf{0} & \mathbf{0} & \mathbf{0} \\ \mathbf{0} & {}^{T}\mathbf{M}^{24} & {}^{T}\mathbf{M}^{34} & \mathbf{M}^{44} & \mathbf{0} & \mathbf{0} & \mathbf{0} \\ {}^{T}\mathbf{M}^{15} & \mathbf{0} & \mathbf{0} & \mathbf{0} & \mathbf{M}^{55} & \mathbf{M}^{56} & \mathbf{M}^{57} \\ {}^{T}\mathbf{M}^{16} & \mathbf{0} & \mathbf{0} & \mathbf{0} & {}^{T}\mathbf{M}^{56} & \mathbf{M}^{66} & \mathbf{M}^{67} \\ {}^{T}\mathbf{M}^{17} & \mathbf{0} & \mathbf{0} & \mathbf{0} & {}^{T}\mathbf{M}^{57} & {}^{T}\mathbf{M}^{67} & \mathbf{M}^{77} \end{bmatrix}\right) \begin{Bmatrix} \mathbf{w} \\ \mathbf{u} \\ \mathbf{v} \\ \mathbf{\Phi} \\ \boldsymbol{\psi}_y \\ \boldsymbol{\psi}_x \\ \boldsymbol{\psi}_{\varpi} \end{Bmatrix} = \begin{Bmatrix} \mathbf{0} \\ \mathbf{0} \\ \mathbf{F} \\ \mathbf{0} \\ \mathbf{0} \\ \mathbf{0} \\ \mathbf{0} \end{Bmatrix} \tag{22}$$

The explicit forms of stiffness matrix **K**, mass matrix **M** and force vector **F** are given in *Appendix A*.

In case of ignoring the shear effect as the classical beam theory, Eqs. (3a)-(3c) degenerate to $\psi_y = -U'$, $\psi_x = -V'$, $\psi_{\varpi} = -\phi'$ and only four unknown variables (W, U, V, ϕ) are available. Thus, the bending, vibration and buckling behaviours of the thin-walled beams in this case can be reduced:

$$\left(\begin{bmatrix} {}_{NS}\mathbf{K}^{11} & {}_{NS}\mathbf{K}^{12} & {}_{NS}\mathbf{K}^{13} & {}_{NS}\mathbf{K}^{14} \\ {}_{NS}^{T}\mathbf{K}^{12} & {}_{NS}\mathbf{K}^{22} & {}_{NS}\mathbf{K}^{23} & {}_{NS}\mathbf{K}^{24} \\ {}_{NS}^{T}\mathbf{K}^{13} & {}_{NS}^{T}\mathbf{K}^{23} & {}_{NS}\mathbf{K}^{33} & {}_{NS}\mathbf{K}^{34} \\ {}_{NS}^{T}\mathbf{K}^{14} & {}_{NS}^{T}\mathbf{K}^{24} & {}_{NS}^{T}\mathbf{K}^{34} & {}_{NS}\mathbf{K}^{44} \end{bmatrix} - \omega^2 \begin{bmatrix} {}_{NS}\mathbf{M}^{11} & \mathbf{0} & \mathbf{0} & \mathbf{0} \\ \mathbf{0} & {}_{NS}\mathbf{M}^{22} & \mathbf{0} & {}_{NS}\mathbf{M}^{24} \\ \mathbf{0} & \mathbf{0} & {}_{NS}\mathbf{M}^{33} & {}_{NS}\mathbf{M}^{34} \\ \mathbf{0} & {}_{NS}^{T}\mathbf{M}^{24} & {}_{NS}^{T}\mathbf{M}^{34} & {}_{NS}\mathbf{M}^{44} \end{bmatrix}\right) \begin{Bmatrix} \mathbf{w} \\ \mathbf{u} \\ \mathbf{v} \\ \mathbf{\Phi} \end{Bmatrix} = \begin{Bmatrix} \mathbf{0} \\ \mathbf{0} \\ {}_{NS}\mathbf{F} \\ \mathbf{0} \end{Bmatrix} \tag{23}$$

The coefficients of the stiffness matrix ${}_{NS}\mathbf{K}$, mass matrix ${}_{NS}\mathbf{M}$ and force vector ${}_{NS}\mathbf{F}$ are given in *Appendix B.*

3. Numerical results

In this section, numerical examples are carried out to show the accuracy of the present solutions and then investigate bending, vibration and buckling behaviours of thin-walled

FG sandwich and composite channel beams. The shear effect is defined as $\left|R_S - R_{NS}\right| / R_S \times 100\%$; where R_{NS} and R_S denote the results from classical and shear deformable theory, respectively. Unless other states, the material and geometry properties used in this section are given as follows:

For FG sandwich channel beams (Fig. 2):

- ✓ *Bending and buckling analysis*: $E_c = 320.7\,GPa$, $E_m = 105.69\,GPa$, $\nu = 0.3$, $h_1 = h_2 = h_3 = h = 0.2\,cm$, $b_1 = b_2 = 20h$, $b_3 = 40h$.
- ✓ *Free vibration analysis*: $E_c = 380\,GPa$, $\rho_c = 3960\,kg/m^3$, $E_m = 70\,GPa$, $\rho_m = 2702\,kg/m^3$, $\nu = 0.3$, $h_1 = h_2 = h_3 = h = 0.5\,cm$, $b_1 = b_2 = 20h$, $b_3 = 40h$.

For composite channel beams (Fig. 3): $E_1 = 53.78\,GPa$, $E_2 = E_3 = 17.93\,GPa$, $G_{12} = G_{13} = 8.96\,GPa$, $G_{23} = 3.45\,GPa$, $\nu_{12} = \nu_{13} = 0.25$, $\rho = 1968.9\,kg/m^3$, $h_1 = h_2 = h_3 = h = 0.208\,cm$, $b_1 = b_2 = 2.5\,cm$, $b_3 = 5\,cm$.

3.1. Convergence study

In order to study convergence of the present solutions, FG sandwich C1-beams ($p = 10$ and $L/b_3 = 20$) and composite channel C4-beams, whose lay-ups in the flanges and web are $\left[30/-30\right]_{4s}$ and $L/b_3 = 20$) subject to a vertical concentrated load ($P_y = 1\,kN$) acting at mid-span with the various BCs are considered. Their mid-span deflections, critical buckling loads and fundamental frequencies are shown in Tables 2 and 3 with various series number m. For all BCs, it can be found that the present solutions converge at $m = 12$ for deflections, and $m = 10$ for critical buckling loads and frequencies. These numbers of series terms will be used in the next sections.

3.2. FG sandwich channel beams

3.2.1. Verification

For bending problem, FG sandwich channel cantilever beams $(L/b_3 = 50)$ with C1-, C2- and C3-sections are considered. The thickness ratio of ceramic material are taken as $(\alpha_1 = \alpha_2 = \alpha_3 = 0.4)$ for C2-section, and $(\alpha_1 = \alpha_2 = 0.9,\ \alpha_3 = 0.1)$ for C3-section. In order to compare with the results of Nguyen, Kim and Lee (2016a), which used classical beam theory, non-dimensional vertical displacement is used as $\overline{V} = \dfrac{E_c h b_3^3}{P_y L^3} V$. Maximum deflections of beams under a vertical load (P_y) acting at free end are shown in Fig. 4. The present results are an excellent agreement with those of Nguyen, Kim and Lee (2016a) for all sections. It is noted that there is not much discrepancy between results of shear and no shear models due to their slenderness $(L/b_3 = 50)$.

In order to verify further, FG sandwich C1-beams ($h_1 = h_2 = h_3 = h = 0.5\,cm$, $b_1 = b_2 = 20h$, $b_3 = 40h$) with $L/b_3 = 12.5$ for buckling and $L/b_3 = 40$ for free vibration are considered. Non-dimensional frequency is defined as $\overline{\omega} = \dfrac{\omega L^2}{b_3}\sqrt{\dfrac{\rho_m}{E_m}}$. Their results are given in Tables 4 and 5, and compared with those from Lanc et al. (2016) and Nguyen, Kim and Lee (2016b), which based on classical beam theory. It is seen that the present results are good agreement with those of previous studies.

3.2.2 Parameter study

3.2.2.1 Bending analysis:

FG sandwich channel beams under a uniform load (q_y = 0.5 *kN/m*) for various BCs, L/b_3 and p are considered to study span-to-height ratio (L/b_3) and material parameter (p). Tables 6-8 show their mid-span deflections with C1-, C2-sections

$(\alpha_1 = \alpha_2 = \alpha_3 = 0.4)$ and C3-section $(\alpha_1 = \alpha_2 = 0.9$ and $\alpha_3 = 0.1)$. It can be seen that they are the largest for C-F and smallest for C-C beams, as expected. Besides, they increase as p increases for all configurations.

The shear effect on the deflections with respect to L/b_3 $(p = 10)$, and with respect to p ($L/b_3 = 10$) are shown Fig. 5 and 6 for C2- and C3-sections. As L/b_3 increases, this effect decreases and has the highest value for C-C beams and the lowest one for C-F beams. For C2-section, it does not depend on material parameter for all BCs (Fig. 5b), which can be explained partly by the constant ratio E_{33}/E_{77} in Fig. 7. However, for C3-section, it strongly increases from $0 \le p \le 5$ after that, increases slowly from $5 \le p \le 40$ as shown in Fig. 6b and again can be justified by ratio (E_{33}/E_{77}).

Next, FG sandwich channel C3-beams under uniform load ($L/b_3 = 10$, $p = 2$ and q_y = 10 *kN/m*) are used to study the shear effect with respect to variation of ceramic's thickness ratio in the flanges and web in Fig. 8. This effect increases as ceramic's thickness ratio in the top and bottom flanges increases, whilst it decreases as ceramic's thickness ratio in the web increases.

3.2.2.2 Vibration and buckling analysis

To investigate shear effect on the critical buckling load and natural frequencies, FG sandwich channel C2-beams ($h_1 = h_2 = h_3 = h = 0.5\,cm$, $b_1 = b_2 = b_3 = 20h$) are considered. Variations of shear effect with respect to L/b_3, ceramic's thickness ratio in flanges (α_1, α_2), web (α_3) and material parameter (p) are showed in Figs. 9 and 10. It can be observed that this effect decreases as ceramic's thickness ratio in flanges increases; increase as ceramic's thickness ratio in web increase, and hardly depend on p. It is significant for higher buckling and vibration modes as shown in Fig. 11.

3.3. Thin-walled composite channel beams

3.3.1. Verification

For bending problem, a cantilever composite channel C4-beam ($L/b_3 = 20$) under a vertical load ($P_y = 1kN$) acting at free end is analysed. This beam is made by 16 layers of symmetric angle-ply lay-ups in the flanges and web. Maximum deflections are given in Table 9 for both shear and no shear case, and compared with results of Kim, Jeon and Lee (2013). Again, the current results are coincided with those from previous research.

For vibration and buckling problems, composite cantilever C4-beams ($h_1 = h_2 = h_3 = h = 0.208\,cm$, $b_1 = b_2 = 2.0\,cm$, $b_3 = 5\,cm$ and $L/b_3 = 20$) are considered. Their results are given in Tables 10 and 11 , and compared with Kim and Lee (2014). It can be seen that there are absolutely coincided between the present results and those of Kim and Lee (2014).

3.3.2 Parameter study

3.3.2.1. Bending analysis

Table 12 presents the mid-span deflections of C4-section beams subjected to a uniform load ($q_y = 0.1kN/m$) for various (L/b_3). Fig. 12 shows the shear effect on the deflection of beams with lay-up $[45/-45]_{4S}$ for various BCs. It can be found that the deflections increase as (L/b_3) and fiber orientation increases.

In order to further examine the shear effect with respect to the fiber orientation, Fig. 13 illustrates the results for C-C composite channel beams ($L/b_3 = 10$, $q_y = 0.1kN/m$) with C5- and C6- sections. The C5-section has the web considered as unidirectional, and the top and bottom flanges assumed to be angle-ply laminates $[\theta/-\theta]$, while the C6-section has the top and bottom flanges considered as unidirectional, and the web assumed to be angle-ply laminates $[\theta / -\theta]$ as shown in Fig. 3. It is clear that the shear effect depends on fiber orientation, and it is stronger for C6-section than C5-section. It is interesting that for C5-section, this effect is minimum at fiber angle $\theta = 60$ whereas for C6-section, it is minimum at $\theta = 40$. This phenomenon is explained in Fig. 14, where (E_{33} / E_{77}) ratio is plotted with respect to fiber orientation.

3.3.2. Vibration and buckling analysis

To investigate shear effect on the critical buckling loads and natural frequencies, composite channel C4-beams ($h_1 = h_2 = h_3 = h = 0.208\,cm$, $b_1 = b_2 = b_3 = 20h$) are considered. Variation of shear effect on critical buckling load and frequency of beams ($[45/-45]_{4S}$ in flanges and web) respect to L/b_3 is plotted in Fig. 15. This effect also depends on fiber angle as shown in Fig. 16. It is more pronounced for higher buckling and vibration modes (Fig. 17).

4. Conclusions

Based on the first-order shear deformation theory, bending, vibration and buckling analysis of thin-walled FG sandwich and composite channel beams is studied. Lagrange's equations are used to formulate the governing equations. Ritz method is developed to obtain the deflections, natural frequencies and buckling loads of thin-walled FG sandwich and composite channel beams. Both results from classical and first-order shear deformation beam theories are derived in a unified fashion. Numerical results are obtained and compared with those available in the literature. Some new results are displayed as benchmark values in the future. The results indicate that the present study is efficient and accurate to analyse the structural responses of FG sandwich and composite channel beams.

Acknowledgements

This research is funded by Vietnam National Foundation for Science and Technology Development (NAFOSTED) under Grant No. 107.02-2018.312.

Appendix A

$$K_{ij}^{11} = E_{11}\int_0^L \varphi_i'' \varphi_j'' dz\,,\quad K_{ij}^{12} = E_{16}\int_0^L \varphi_i'' \varphi_j' dz\,,\quad K_{ij}^{13} = E_{17}\int_0^L \varphi_i'' \varphi_j' dz\,,\quad K_{ij}^{14} = \left(E_{15} + E_{18}\right)\int_0^L \varphi_i'' \varphi_j' dz\,,$$

$$K_{ij}^{15} = E_{12}\int_0^L \varphi_i'' \varphi_j'' dz + E_{16}\int_0^L \varphi_i' \varphi_j dz\,,\quad K_{ij}^{16} = E_{13}\int_0^L \varphi_i'' \varphi_j'' dz + E_{17}\int_0^L \varphi_i'' \varphi_j' dz\,,$$

$$K_{ij}^{17} = E_{14}\int_0^L \varphi_i'' \varphi_j'' dz + \left(E_{18} - E_{15}\right)\int_0^L \varphi_i'' \varphi_j' dz\,,\quad K_{ij}^{22} = E_{66}\int_0^L \varphi_i' \varphi_j' dz - N_0\int_0^L \varphi_i' \varphi_j' dz\,,\quad K_{ij}^{23} = E_{67}\int_0^L \varphi_i' \varphi_j' dz\,,$$

$$K_{ij}^{24} = \left(E_{56} + E_{68}\right)\int_0^L \varphi_i' \varphi_j' dz - N_0 y_p\int_0^L \varphi_i' \varphi_j' dz\,,\quad K_{ij}^{25} = E_{26}\int_0^L \varphi_i' \varphi_j'' dz + E_{66}\int_0^L \varphi_i' \varphi_j' dz\,,$$

$$K_{ij}^{26} = E_{36}\int_0^L \varphi_i' \varphi_j'' dz + E_{67}\int_0^L \varphi_i' \varphi_j' dz\,,\quad K_{ij}^{27} = E_{46}\int_0^L \varphi_i' \varphi_j'' dz + \left(E_{68} - E_{56}\right)\int_0^L \varphi_i' \varphi_j' dz\,,$$

$$K_{ij}^{33} = E_{77}\int_0^L \varphi_i' \varphi_j' dz - N_0\int_0^L \varphi_i' \varphi_j' dz\,,\quad K_{ij}^{34} = \left(E_{57} + E_{78}\right)\int_0^L \varphi_i' \varphi_j' dz + N_0 x_p\int_0^L \varphi_i' \varphi_j' dz\,,$$

$$K_{ij}^{35} = E_{27}\int_0^L \varphi_i' \varphi_j'' dz + E_{67}\int_0^L \varphi_i' \varphi_j' dz\,,\quad K_{ij}^{36} = E_{37}\int_0^L \varphi_i' \varphi_j'' dz + E_{77}\int_0^L \varphi_i' \varphi_j' dz\,,$$

$$K_{ij}^{37} = E_{47}\int_0^L \varphi_i' \varphi_j'' dz + \left(E_{78} - E_{57}\right)\int_0^L \varphi_i' \varphi_j' dz\,,\quad K_{ij}^{44} = \left(E_{55} + 2E_{58} + E_{88}\right)\int_0^L \varphi_i' \varphi_j' dz - \frac{N_0 I_p}{A}\int_0^L \varphi_i' \varphi_j' dz\,,$$

$$K_{ij}^{45} = \left(E_{25} + E_{28}\right)\int_0^L \varphi_i' \varphi_j'' dz + \left(E_{56} + E_{68}\right)\int_0^L \varphi_i' \varphi_j' dz\,,$$

$$K_{ij}^{46} = \left(E_{35} + E_{38}\right)\int_0^L \varphi_i' \varphi_j'' dz + \left(E_{57} + E_{78}\right)\int_0^L \varphi_i' \varphi_j' dz\,,$$

$$K_{ij}^{47} = \left(E_{45} + E_{48}\right)\int_0^L \varphi_i' \varphi_j'' dz + \left(E_{88} - E_{55}\right)\int_0^L \varphi_i' \varphi_j' dz\,,$$

$$K_{ij}^{55} = E_{22}\int_0^L \varphi_i'' \varphi_j'' dz + E_{26}\int_0^L \left(\varphi_i'' \varphi_j' + \varphi_i' \varphi_j''\right) dz + E_{66}\int_0^L \varphi_i' \varphi_j' dz\,,$$

$$K_{ij}^{56}=E_{23}\int_0^L \varphi_i''\varphi_j''dz+E_{27}\int_0^L \varphi_i''\varphi_j'dz+E_{36}\int_0^L \varphi_i'\varphi_j''dz+E_{67}\int_0^L \varphi_i'\varphi_j'dz\,,$$

$$K_{ij}^{57}=E_{24}\int_0^L \varphi_i''\varphi_j''dz+\left(E_{28}-E_{25}\right)\int_0^L \varphi_i''\varphi_j'dz+E_{46}\int_0^L \varphi_i'\varphi_j''dz+\left(E_{68}-E_{56}\right)\int_0^L \varphi_i'\varphi_j'dz\,,$$

$$K_{ij}^{66}=E_{33}\int_0^L \varphi_i''\varphi_j''dz+E_{37}\int_0^L \left(\varphi_i''\varphi_j'+\varphi_i'\varphi_j''\right)dz+E_{77}\int_0^L \varphi_i'\varphi_j'dz\,,$$

$$K_{ij}^{67}=E_{34}\int_0^L \varphi_i''\varphi_j''dz+\left(E_{38}-E_{35}\right)\int_0^L \varphi_i''\varphi_j'dz+E_{47}\int_0^L \varphi_i'\varphi_j''dz+\left(E_{78}-E_{57}\right)\int_0^L \varphi_i'\varphi_j'dz\,,$$

$$K_{ij}^{77}=E_{44}\int_0^L \varphi_i''\varphi_j''dz+\left(E_{48}-E_{45}\right)\int_0^L \left(\varphi_i''\varphi_j'+\varphi_i'\varphi_j''\right)dz+\left(E_{88}-2E_{58}+E_{55}\right)\int_0^L \varphi_i'\varphi_j'dz\,, \tag{A1}$$

$$F_i=\int_0^L q_y\varphi_j dz+P_y\varphi_j\left(z_L\right) \tag{A2}$$

$$M_{ij}^{11}=m_0\int_0^L \varphi_i'\varphi_j'dz\,,\quad M_{ij}^{15}=m_s\int_0^L \varphi_i'\varphi_j'dz\,,\quad M_{ij}^{16}=-m_c\int_0^L \varphi_i'\varphi_j'dz\,,\quad M_{ij}^{17}=\left(m_{\varpi}-m_q\right)\int_0^L \varphi_i'\varphi_j'dz\,,$$

$$M_{ij}^{22}=m_0\int_0^L \varphi_i\varphi_j dz\,,\quad M_{ij}^{24}=\left(m_c+m_0y_p\right)\int_0^L \varphi_i\varphi_j dz\,,\quad M_{ij}^{33}=m_0\int_0^L \varphi_i\varphi_j dz\,,$$

$$M_{ij}^{34}=\left(m_s-m_0x_p\right)\int_0^L \varphi_i\varphi_j dz\,,\quad M_{ij}^{44}=\left(m_p+m_2+2m_r\right)\int_0^L \varphi_i\varphi_j dz\,,$$

$$M_{ij}^{55}=\left(m_{x2}+2m_{xs}+m_{s2}\right)\int_0^L \varphi_i'\varphi_j'dz\,,\quad M_{ij}^{56}=\left(m_{xycs}-m_{cs}\right)\int_0^L \varphi_i'\varphi_j'dz\,,$$

$$M_{ij}^{57}=\left(m_{x\varpi}+m_{x\varpi qs}-m_{qs}\right)\int_0^L \varphi_i'\varphi_j'dz\,,\quad M_{ij}^{66}=\left(m_{y2}-2m_{yc}+m_{c2}\right)\int_0^L \varphi_i'\varphi_j'dz\,,$$

$$M_{ij}^{67}=\left(m_{y\varpi}-m_{y\varpi qc}+m_{qc}\right)\int_0^L \varphi_i'\varphi_j'dz\,,\quad M_{ij}^{77}=\left(m_{\varpi 2}-2m_{q\varpi}+m_{q2}\right)\int_0^L \varphi_i'\varphi_j'dz \tag{A3}$$

Appendix B

$${}_{NS}K_{ij}^{11}=E_{11}\int_0^L \varphi_i''\varphi_j''dz\,,\quad {}_{NS}K_{ij}^{12}=-E_{12}\int_0^L \varphi_i''\varphi_j''dz\,,\quad {}_{NS}K_{ij}^{13}=-E_{13}\int_0^L \varphi_i''\varphi_j''dz\,,$$

$$ {}_{NS}K_{ij}^{14} = 2E_{15}\int_0^L \varphi_i^{''}\varphi_j^{'}dz - E_{14}\int_0^L \varphi_i^{''}\varphi_j^{''}dz \,, \quad {}_{NS}K_{ij}^{22} = E_{22}\int_0^L \varphi_i^{''}\varphi_j^{''}dz - N_0\int_0^L \varphi_i^{'}\varphi_j^{'}dz \,, {}_{NS}K_{ij}^{23} = E_{23}\int_0^L \varphi_i^{''}\varphi_j^{''}dz \,, $$

$$ {}_{NS}K_{ij}^{24} = E_{24}\int_0^L \varphi_i^{''}\varphi_j^{''}dz - 2E_{25}\int_0^L \varphi_i^{''}\varphi_j^{'}dz - N_0 y_p\int_0^L \varphi_i^{'}\varphi_j^{'}dz \,, \quad {}_{NS}K_{ij}^{33} = E_{33}\int_0^L \varphi_i^{''}\varphi_j^{''}dz - N_0\int_0^L \varphi_i^{'}\varphi_j^{'}dz \,, $$

$$ {}_{NS}K_{ij}^{34} = E_{34}\int_0^L \varphi_i^{''}\varphi_j^{''}dz - 2E_{35}\int_0^L \varphi_i^{''}\varphi_j^{'}dz + N_0 x_p\int_0^L \varphi_i^{'}\varphi_j^{'}dz \,, $$

$$ {}_{NS}K_{ij}^{44} = E_{44}\int_0^L \varphi_i^{''}\varphi_j^{''}dz - 2E_{45}\left(\int_0^L \varphi_i^{''}\varphi_j^{'}dz + \int_0^L \varphi_i^{'}\varphi_j^{''}dz\right) + 4E_{55}\int_0^L \varphi_i^{'}\varphi_j^{'}dz - \frac{N_0 I_p}{A}\int_0^L \varphi_i^{'}\varphi_j^{'}dz \,, \tag{B1} $$

$$ {}_{NS}F_i = \int_0^L q_y\varphi_j dz + P_y\varphi_j\left(z_L\right) \tag{B2} $$

$$ {}_{NS}M_{ij}^{11} = m_0\int_0^L \varphi_i^{'}\varphi_j^{'}dz \,, \quad {}_{NS}M_{ij}^{22} = m_0\int_0^L \varphi_i\varphi_j dz \,, \quad {}_{NS}M_{ij}^{24} = \left(m_c + m_0 y_p\right)\int_0^L \varphi_i\varphi_j dz \,, $$

$$ {}_{NS}M_{ij}^{33} = m_0\int_0^L \varphi_i\varphi_j dz \,, \quad {}_{NS}M_{ij}^{34} = \left(m_s - m_0 x_p\right)\int_0^L \varphi_i\varphi_j dz \,, {}_{NS}M_{ij}^{44} = \left(m_p + m_2 + 2m_{\varpi}\right)\int_0^L \varphi_i\varphi_j dz \tag{B3} $$

References

Aguiar, R., F. Moleiro and C. M. Soares (2012). "Assessment of mixed and displacement-based models for static analysis of composite beams of different cross-sections." Composite Structures **94**(2): 601-616.DOI: https://doi.org/10.1016/j.compstruct.2011.08.028.

Alizada, A., A. Sofiyev and N. Kuruoglu (2012). "Stress analysis of a substrate coated by nanomaterials with vacancies subjected to uniform extension load." Acta Mechanica **223**(7): 1371-1383.DOI: https://doi.org/10.1007/s00707-012-0649-5

Arnaud, L., O. Gonzalo, S. Seguy, H. Jauregi and G. Peigné (2011). "Simulation of low rigidity part machining applied to thin-walled structures." The International

Journal of Advanced Manufacturing Technology **54**(5-8): 479-488.DOI: https://doi.org/10.1007/s00170-010-2976-9.

Ascione, L., L. Feo and G. Mancusi (2000). "On the statical behaviour of fibre-reinforced polymer thin-walled beams." Composites Part B: Engineering **31**(8): 643-654.DOI: https://doi.org/10.1016/S1359-8368(00)00032-9.

Aydogdu, M. (2006a). "Buckling analysis of cross-ply laminated beams with general boundary conditions by Ritz method." Composites Science and Technology **66**(10): 1248-1255.DOI: https://doi.org/10.1016/j.compscitech.2005.10.029.

Aydogdu, M. (2006b). "Free vibration analysis of angle-ply laminated beams with general boundary conditions." Journal of reinforced plastics and composites **25**(15): 1571-1583.DOI: https://doi.org/10.1177/0731684406066752.

Back, S. Y. and K. M. Will (2008). "Shear-flexible thin-walled element for composite I-beams." Engineering Structures **30**(5): 1447-1458.DOI: https://doi.org/10.1016/j.engstruct.2007.08.002.

Bauld, N. R. and T. Lih-Shyng (1984). "A Vlasov theory for fiber-reinforced beams with thin-walled open cross sections." International Journal of Solids and Structures **20**(3): 277-297.DOI: https://doi.org/10.1016/0020-7683(84)90039-8.

Cárdenas, D., H. Elizalde, J. C. Jáuregui-Correa, M. T. Piovan and O. Probst (2018). "Unified theory for curved composite thin-walled beams and its isogeometrical analysis." Thin-Walled Structures **131**: 838-854.DOI: https://doi.org/10.1016/j.tws.2018.07.036.

Cortínez, V. H. and M. T. Piovan (2006). "Stability of composite thin-walled beams with shear deformability." Computers & structures **84**(15-16): 978-990.DOI: https://doi.org/10.1016/j.compstruc.2006.02.017.

Dechao, Z., D. Zhongmin and W. Xingwei (2001). "The analysis of thin walled composite laminated helicopter rotor with hierarchical warping functions and finite element method." Acta Mechanica Sinica **17**(3): 258-268.DOI: https://doi.org/10.1007/BF02486882.

Günay, M. G. and T. Timarci (2017). "Static analysis of thin-walled laminated composite closed-section beams with variable stiffness." Composite Structures **182**: 67-78.DOI: https://doi.org/10.1016/j.compstruct.2017.08.092.

Harursampath, D., A. B. Harish and D. H. Hodges (2017a). "Model reduction in thin-walled open-section composite beams using variational asymptotic method. Part I: Theory." Thin-Walled Structures **117**: 356-366.DOI: https://doi.org/10.1016/j.tws.2017.03.018.

Harursampath, D., A. B. Harish and D. H. Hodges (2017b). "Model reduction in thin-walled open-section composite beams using Variational Asymptotic Method. Part II: Applications." Thin-Walled Structures **117**: 367-377.DOI: https://doi.org/10.1016/j.tws.2017.03.021.

Kim, N.-I. (2011). "Shear deformable doubly-and mono-symmetric composite I-beams." International Journal of mechanical sciences **53**(1): 31-41.DOI: https://doi.org/10.1016/j.ijmecsci.2010.10.004.

Kim, N.-I. (2012). "Shear deformable composite beams with channel-section on elastic foundation." European Journal of Mechanics-A/Solids **36**: 104-121.DOI: https://doi.org/10.1016/j.euromechsol.2012.02.003.

Kim, N.-I. and C.-K. Jeon (2013). "Coupled Static and Dynamic Analyses of Shear Deformable Composite Beams with Channel-Sections." Mechanics Based Design of Structures and Machines **41**(4): 489-511.DOI:

https://doi.org/10.1080/15397734.2013.797332.

Kim, N.-I., C.-K. Jeon and J. Lee (2013). "A new laminated composite beam element based on eigenvalue problem." European Journal of Mechanics-A/Solids **41**: 111-122.DOI: https://doi.org/10.1016/j.euromechsol.2013.02.004.

Kim, N.-I. and J. Lee (2014). "Exact solutions for stability and free vibration of thin-walled Timoshenko laminated beams under variable forces." Archive of Applied Mechanics **84**(12).DOI: https://doi.org/10.1007/s00419-014-0886-2.

Kim, N.-I. and J. Lee (2015). "Refined Series Methodology for the Fully Coupled Thin-Walled Laminated Beams Considering Foundation Effects." Mechanics Based Design of Structures and Machines **43**(2): 125-149.DOI: https://doi.org/10.1080/15397734.2014.931811.

Kim, N.-I. and J. Lee (2017a). "Exact solutions for coupled responses of thin-walled FG sandwich beams with non-symmetric cross-sections." Composites Part B: Engineering **122**: 121-135.DOI: https://doi.org/10.1016/j.compositesb.2017.04.016.

Kim, N.-I. and J. Lee (2017b). "Flexural-torsional analysis of functionally graded sandwich I-beams considering shear effects." Composites Part B: Engineering **108**: 436-450.DOI: https://doi.org/10.1016/j.compositesb.2016.09.092.

Kim, N.-I. and J. Lee (2018). "Nonlinear analysis of thin-walled Al/Al2O3 FG sandwich I-beams with mono-symmetric cross-section." European Journal of Mechanics-A/Solids **69**: 55-70.DOI: https://doi.org/10.1016/j.euromechsol.2017.11.010.

Kim, N.-I. and D. K. Shin (2009). "Coupled deflection analysis of thin-walled Timoshenko laminated composite beams." Computational Mechanics **43**(4): 493.DOI: https://doi.org/10.1007/s00466-008-0324-9.

Kim, N.-I., D. K. Shin and M.-Y. Kim (2006). "Exact solutions for thin-walled open-section composite beams with arbitrary lamination subjected to torsional moment." Thin-walled structures **44**(6): 638-654.DOI: https://doi.org/10.1016/j.tws.2006.05.001.

Kollár, L. P. and A. Pluzsik (2012). "Bending and torsion of composite beams (torsional-warping shear deformation theory)." Journal of Reinforced Plastics and Composites **31**(7): 441-480.DOI: https://doi.org/10.1177/0731684412437611.

Lanc, D., G. Turkalj, T. P. Vo and J. Brnić (2016). "Nonlinear buckling behaviours of thin-walled functionally graded open section beams." Composite Structures **152**: 829-839.DOI: https://doi.org/10.1016/j.compstruct.2016.06.023.

Lee, J. (2001). "Center of gravity and shear center of thin-walled open-section composite beams." Composite structures **52**(2): 255-260.DOI: https://doi.org/10.1016/S0263-8223(00)00177-X.

Lee, J. (2005). "Flexural analysis of thin-walled composite beams using shear-deformable beam theory." Composite Structures **70**(2): 212-222.DOI: https://doi.org/10.1016/j.compstruct.2004.08.023.

Li, C., H.-S. Shen and H. Wang (2019a). "Nonlinear bending of sandwich beams with functionally graded negative Poisson’s ratio honeycomb core." Composite Structures **212**: 317-325.DOI:https://doi.org/10.1016/j.compstruct.2019.01.020

Li, C., H.-S. Shen and H. Wang (2019b). "Nonlinear dynamic response of sandwich beams with functionally graded negative Poisson’s ratio honeycomb core." The European Physical Journal Plus **134**(2): 1-15. DOI: https://doi.org/10.1140/epjp/i2019-12572-7

Li, C., H.-S. Shen and H. Wang (2019c). "Nonlinear vibration of sandwich beams with functionally graded negative Poisson’s ratio honeycomb core." International Journal of Structural Stability and Dynamics **19**(03): 1950034. DOI: https://doi.org/10.1142/S0219455419500342

Li, C., H.-S. Shen and H. Wang (2019d). "Thermal post-buckling of sandwich beams with functionally graded negative Poisson's ratio honeycomb core." International Journal of Mechanical Sciences **152**: 289-297.DOI: https://doi.org/10.1016/j.ijmecsci.2019.01.002

Librescu, L. and O. Song (2005). Thin-walled composite beams: theory and application, Springer Science & Business Media.

Maceri, F. and G. Vairo (2009). "Anisotropic thin-walled beam models: A rational deduction from three-dimensional elasticity." Journal of Mechanics of Materials and Structures **4**(2): 371-394.DOI: DOI: 10.2140/jomms.2009.4.371.

Malekshahi, A., M. Hosseini and A. N. Ansari (2020). "Theoretical estimation of axial crushing behavior of multicell hollow sections." Mechanics Based Design of Structures and Machines: 1-25.DOI: https://doi.org/10.1080/15397734.2020.1776133.

Mantari, J. and F. Canales (2016). "Free vibration and buckling of laminated beams via hybrid Ritz solution for various penalized boundary conditions." Composite Structures **152**: 306-315.DOI: https://doi.org/10.1016/j.compstruct.2016.05.037.

Mao, R. and Q. Lin (1996). "BUCKLING AND INITIAL POST-BUCKLING OF THIN-WALLED COMPOSITE BEAMS." Mechanics of Composite Materials and Structures **3**(3): 201-223.DOI: 10.1080/10759419608945864.

Moon, C.-J., I.-H. Kim, B.-H. Choi, J.-H. Kweon and J.-H. Choi (2010). "Buckling of filament-wound composite cylinders subjected to hydrostatic pressure for underwater vehicle applications." Composite structures **92**(9): 2241-2251.DOI: https://doi.org/10.1016/j.compstruct.2009.08.005.

Nguyen, N.-D., T.-K. Nguyen, T. P. Vo, T.-N. Nguyen and S. Lee (2019). "Vibration and buckling behaviours of thin-walled composite and functionally graded sandwich I-beams." Composites Part B: Engineering **166**: 414-427.DOI: https://doi.org/10.1016/j.compositesb.2019.02.033.

Nguyen, T.-K., N.-D. Nguyen, T. P. Vo and H.-T. Thai (2017). "Trigonometric-series solution for analysis of laminated composite beams." Composite Structures **160**: 142-151.DOI: https://doi.org/10.1016/j.compstruct.2016.10.033.

Nguyen, T.-T., N.-I. Kim and J. Lee (2016a). "Analysis of thin-walled open-section beams with functionally graded materials." Composite Structures **138**: 75-83.DOI: https://doi.org/10.1016/j.compstruct.2015.11.052.

Nguyen, T.-T., N.-I. Kim and J. Lee (2016b). "Free vibration of thin-walled functionally graded open-section beams." Composites Part B: Engineering **95**: 105-116.DOI: https://doi.org/10.1016/j.compositesb.2016.03.057.

Pagani, A., E. Carrera and A. J. M. Ferreira (2016). "Higher-order theories and radial basis functions applied to free vibration analysis of thin-walled beams." Mechanics of Advanced Materials and Structures **23**(9): 1080-1091.DOI: 10.1080/15376494.2015.1121555.

Pavazza, R., A. Matoković and M. Vukasović (2020). "A theory of torsion of thin-walled beams of arbitrary open sections with influence of shear." Mechanics Based Design of Structures and Machines: 1-36.DOI: https://doi.org/10.1080/15397734.2020.1714449.

Pawar, P. M. and R. Ganguli (2006). "Modeling progressive damage accumulation in thin walled composite beams for rotor blade applications." Composites science and technology **66**(13): 2337-2349.DOI: https://doi.org/10.1016/j.compscitech.2005.11.033.

Pradhan, K. and S. Chakraverty (2013). "Free vibration of Euler and Timoshenko functionally graded beams by Rayleigh–Ritz method." Composites Part B: Engineering **51**: 175-184.DOI: https://doi.org/10.1016/j.compositesb.2013.02.027.

Qiao, P. and G. Zou (2002). "Free Vibration Analysis of Fiber-Reinforced Plastic Composite Cantilever I-Beams." Mechanics of Advanced Materials and Structures **9**(4): 359-373.DOI: 10.1080/15376490290096991.

Reddy, J. N. (2003). Mechanics of laminated composite plates and shells: theory and analysis, CRC press.

Sheikh, A. H. and O. T. Thomsen (2008). "An efficient beam element for the analysis of laminated composite beams of thin-walled open and closed cross sections." Composites Science and Technology **68**(10): 2273-2281.DOI: https://doi.org/10.1016/j.compscitech.2008.04.018.

Shin, D. K., N.-I. Kim and M.-Y. Kim (2007). "Exact stiffness matrix of mono-symmetric composite I-beams with arbitrary lamination." Composite structures **79**(4): 467-480.DOI: https://doi.org/10.1016/j.compstruct.2006.02.005.

Şimşek, M. (2009). "Static analysis of a functionally graded beam under a uniformly distributed load by Ritz method." Int J Eng Appl Sci **1**(3): 1-11.

Sofiyev, A. (2014). "The vibration and buckling of sandwich cylindrical shells covered by different coatings subjected to the hydrostatic pressure." Composite Structures **117**: 124-134.DOI: https://doi.org/10.1016/j.compstruct.2014.06.025.

Sofiyev, A. (2019). "Review of research on the vibration and buckling of the FGM conical shells." Composite Structures **211**: 301-317.DOI: https://doi.org/10.1016/j.compstruct.2018.12.047.

Sofiyev, A., D. Hui, S. Huseynov, M. Salamci and G. Yuan (2016a). "Stability and vibration of sandwich cylindrical shells containing a functionally graded material core with transverse shear stresses and rotary inertia effects." Proceedings of the Institution of Mechanical Engineers, Part C: Journal of Mechanical Engineering Science **230**(14): 2376-2389.DOI: https://doi.org/10.1177/0954406215593570.

Sofiyev, A. and E. Osmancelebioglu (2017). "The free vibration of sandwich truncated conical shells containing functionally graded layers within the shear deformation theory." Composites Part B: Engineering **120**: 197-211.DOI: https://doi.org/10.1016/j.compositesb.2017.03.054

Sofiyev, A. H., D. Hui, A. Valiyev, F. Kadioglu, S. Turkaslan, G. Yuan, V. Kalpakci and A. Özdemir (2016b). "Effects of shear stresses and rotary inertia on the stability and vibration of sandwich cylindrical shells with FGM core surrounded by elastic medium." Mechanics Based Design of Structures and Machines **44**(4): 384-404.DOI: https://doi.org/10.1080/15397734.2015.1083870.

Vlasov, V. (1961). Thin-walled elastic beams. Israel program for scientific translations, Jerusalem, Oldbourne Press, London.

Vo, T. P. and J. Lee (2009). "Flexural–torsional coupled vibration and buckling of thin-walled open section composite beams using shear-deformable beam theory." International Journal of Mechanical Sciences **51**(9): 631-641.DOI: https://doi.org/10.1016/j.ijmecsci.2009.05.001.

Vo, T. P. and J. Lee (2013). "Vibration and buckling of thin-walled composite I-beams with arbitrary lay-ups under axial loads and end moments." Mechanics of

Advanced Materials and Structures **20**(8): 652-665.DOI: https://doi.org/10.1080/15376494.2011.643284.

Xu, F., X. Zhang and H. Zhang (2018). "A review on functionally graded structures and materials for energy absorption." Engineering Structures **171**: 309-325.DOI: https://doi.org/10.1016/j.engstruct.2018.05.094.

Zhu, Z., L. Zhang, D. Zheng and G. Cao (2016). "Free vibration of horizontally curved thin-walled beams with rectangular hollow sections considering two compatible displacement fields." Mechanics Based Design of Structures and Machines **44**(4): 354-371.DOI: https://doi.org/10.1080/15397734.2015.1075410.

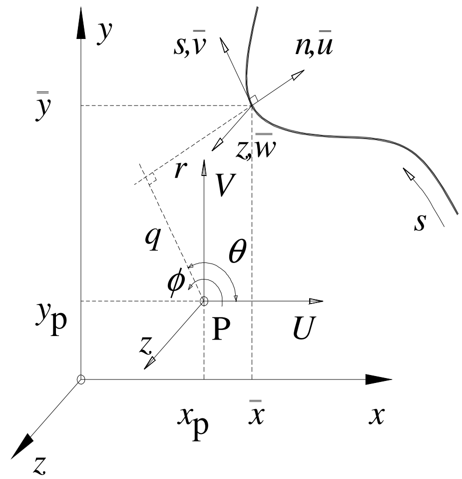

Figure 1. Thin-walled coordinate systems.

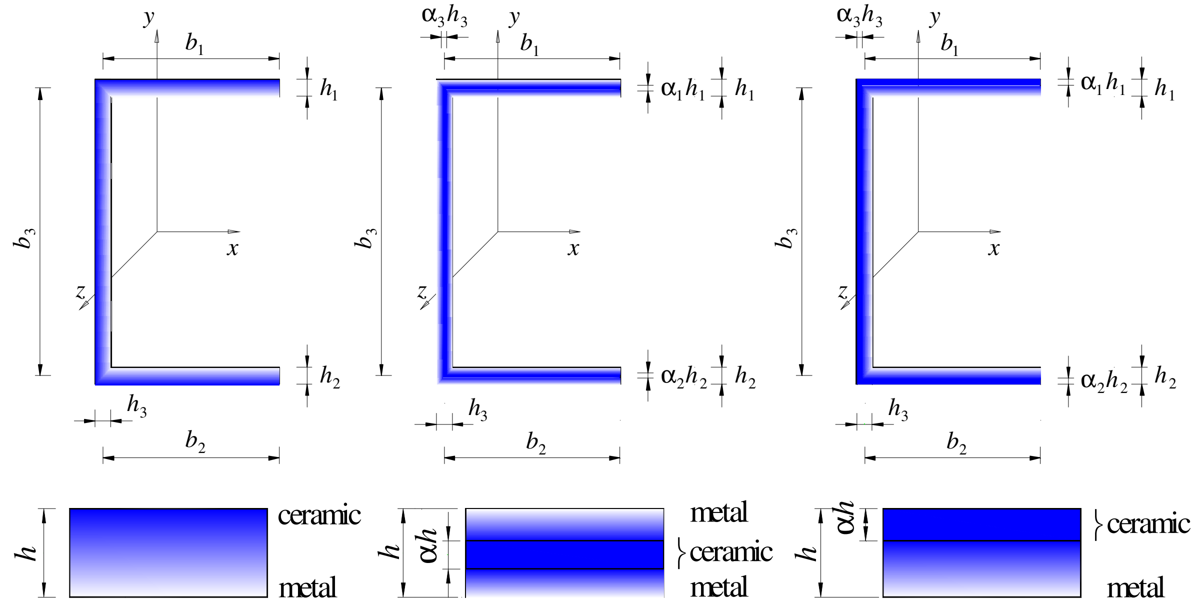

Figure 2. Three cross-sections and material distributions of thin-walled FG sandwich channel beams.

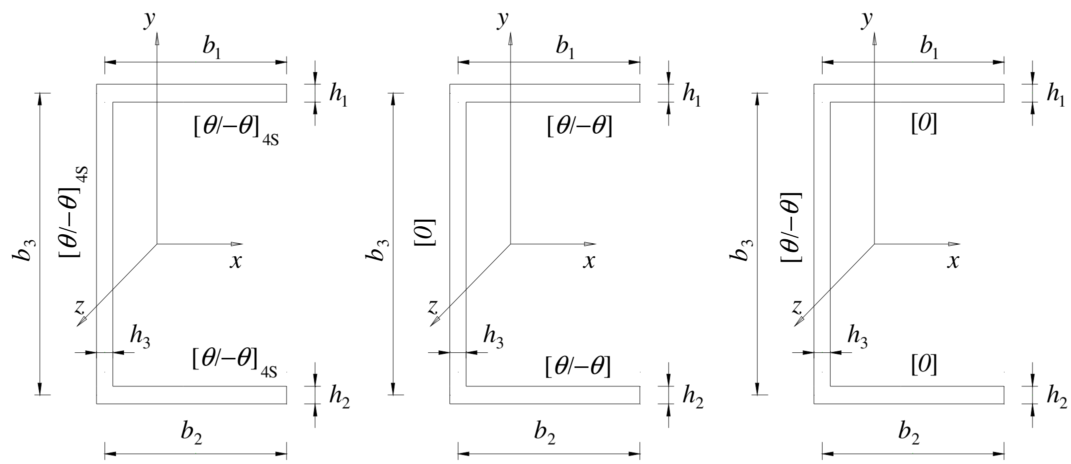

C4-section C5-section C6-section

Figure 3. Three cross-section of thin-walled composite channel beams.

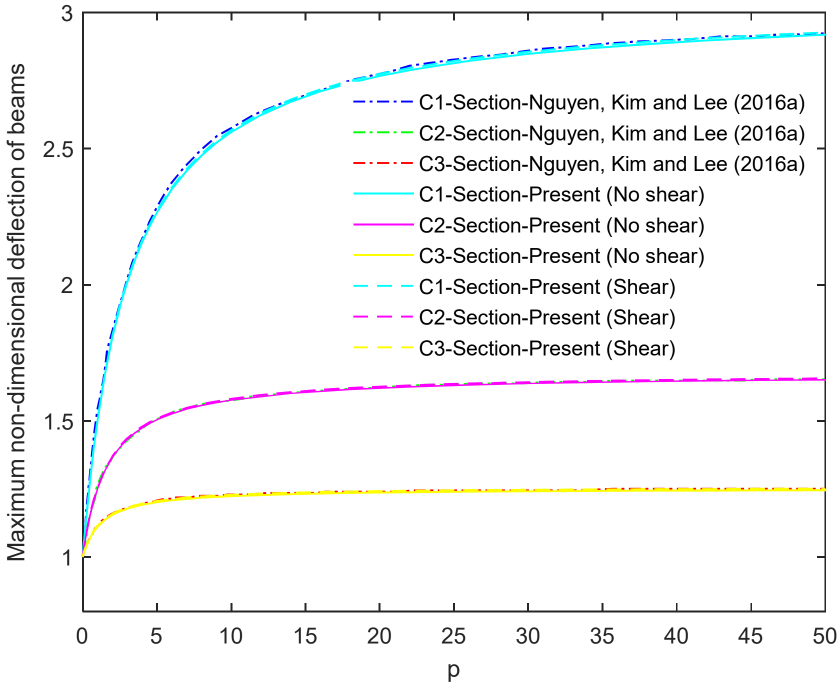

Figure 4. Maximum non-dimensional deflections of FG sandwich cantilever beams.

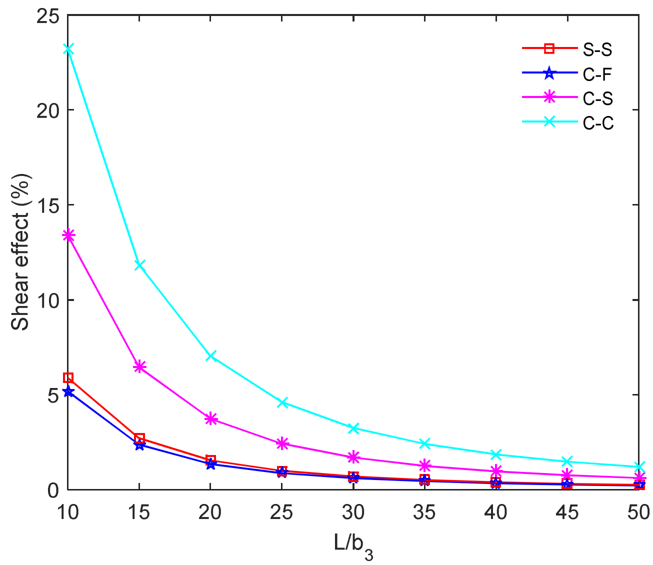

a. $\alpha_1 = \alpha_2 = \alpha_3 = 0.4$ and $p = 10$

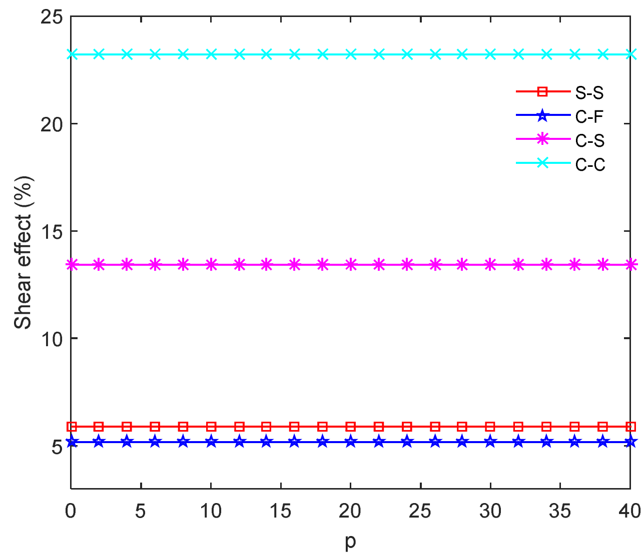

b. $\alpha_1 = \alpha_2 = \alpha_3 = 0.4$ and $L/b_3 = 10$

Figure 5. Shear effect on the deflections of FG sandwich C2-beams with respect to L/b_3 and p for various BCs.

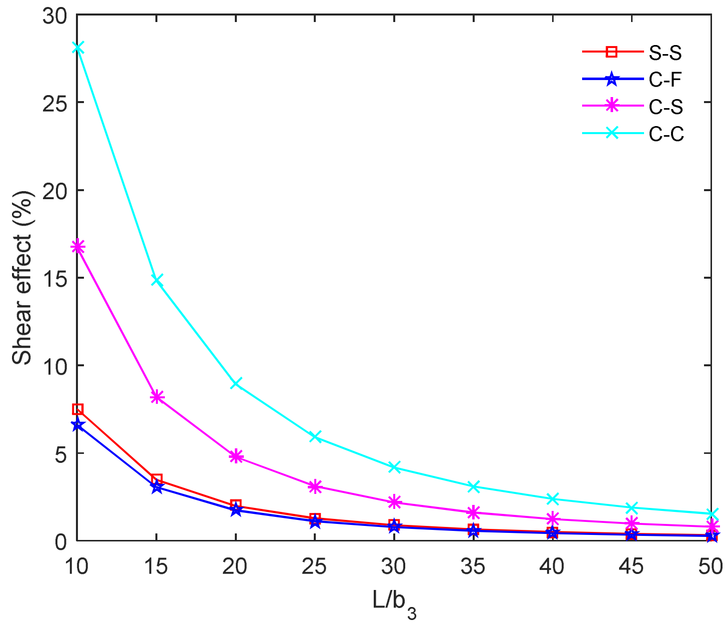

a. $\alpha_1 = \alpha_2 = 0.9$, $\alpha_3 = 0.1$ and $p = 10$

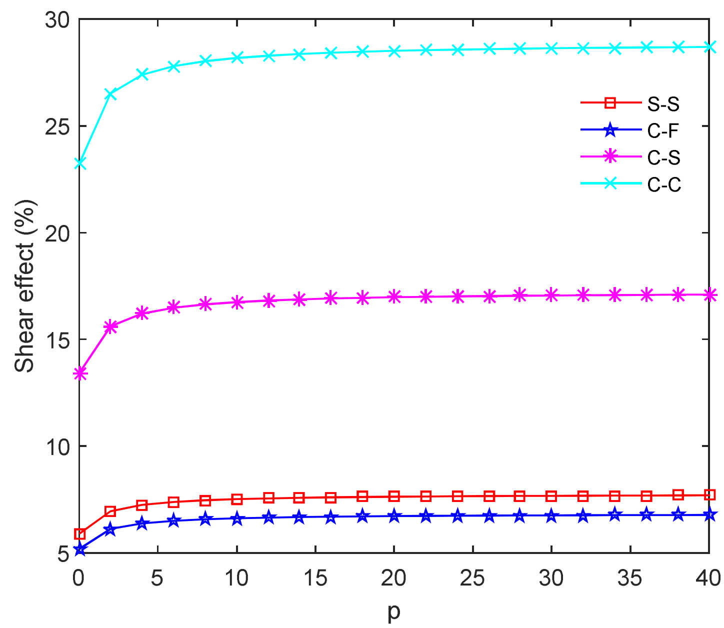

b. $\alpha_1 = \alpha_2 = 0.9$, $\alpha_3 = 0.1$ and $L/b_3 = 10$

Figure 6. Shear effect on the deflections of FG sandwich C3-beams with respect to L/b_3 and p for various BCs.

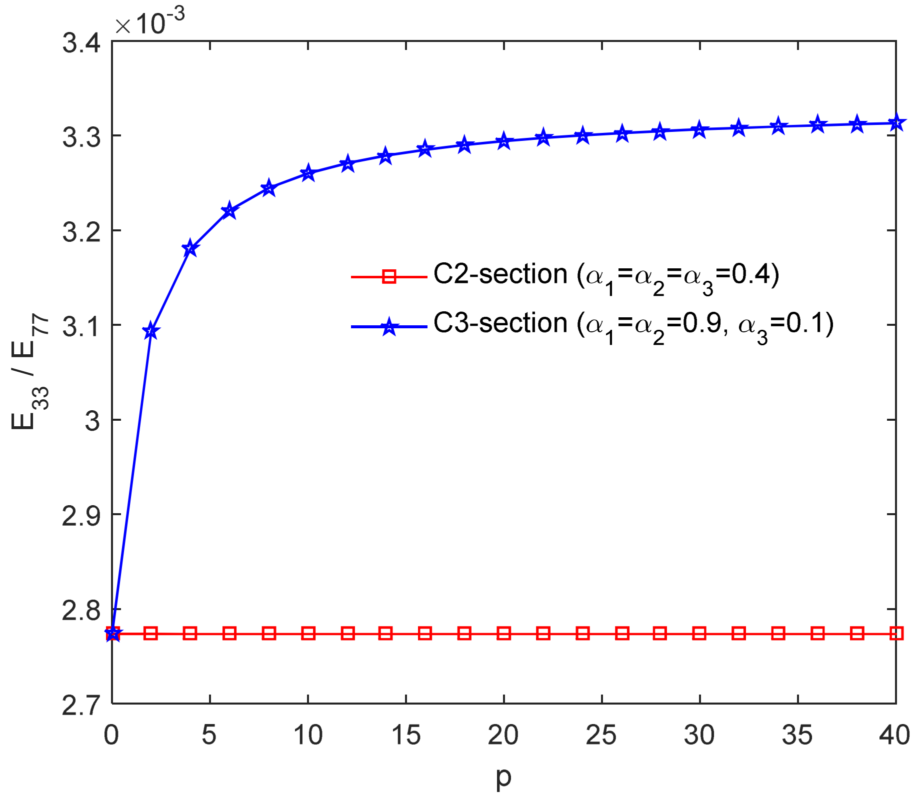

Figure 7. E_{33} / E_{77} ratio of FG sandwich beams for C2- and C3-section with respect to material parameter.

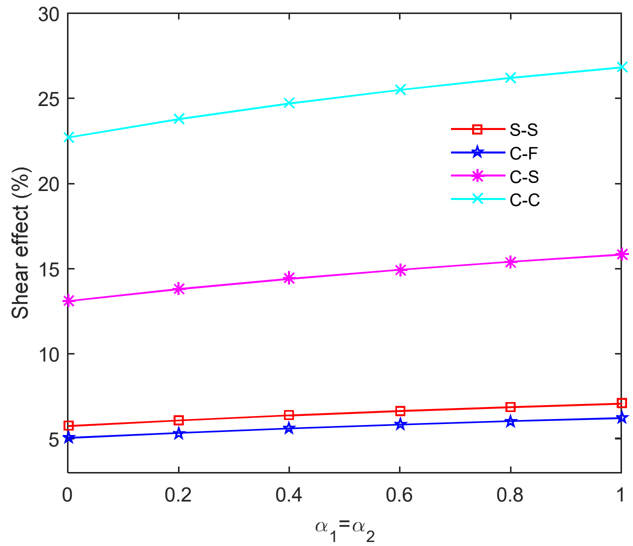

a. $\alpha_3 = 0.1$, $p = 2$ with respect to $\alpha_1 = \alpha_2$

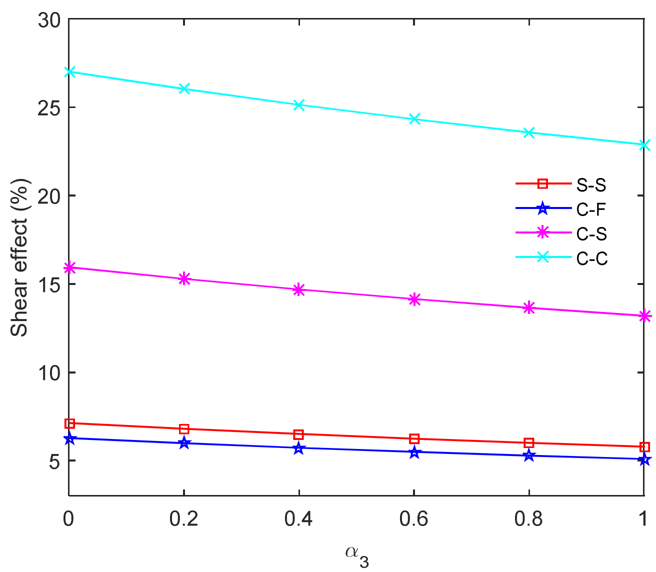

b. $\alpha_1 = \alpha_2 = 0.9$, $p = 2$ with respect to α_3

Figure 8. Shear effect on the deflections of FG sandwich C3-beams ($L/b_3 = 10$) with respect to ceramic's thickness ratio of top and bottom flanges $(\alpha_3 = 0.1, \alpha_1 = \alpha_2)$ and ceramic's thickness ratio of web $(\alpha_1 = \alpha_2 = 0.9, \alpha_3)$.

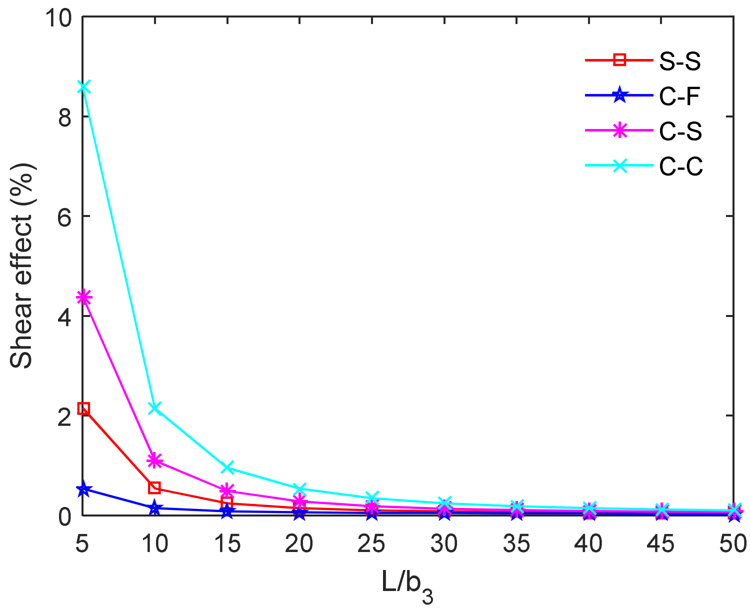

a. Critical buckling load

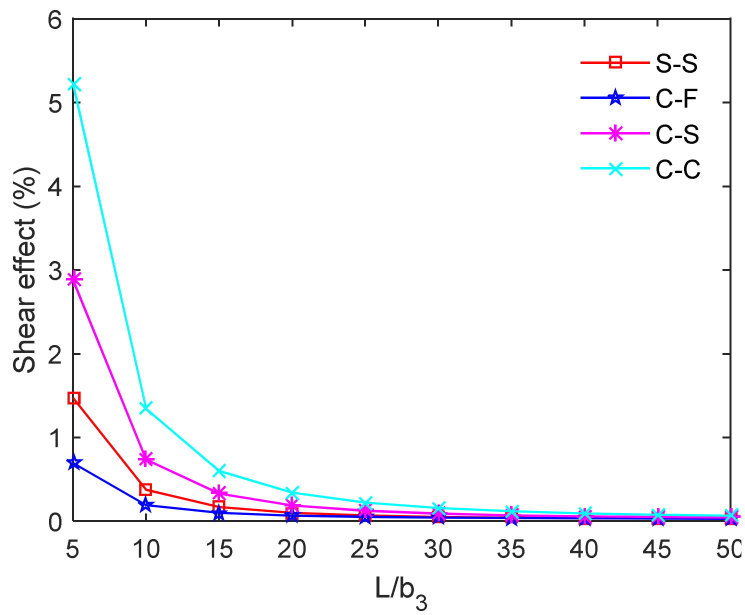

b. Fundamental frequency

Figure 9. Shear effect on the critical buckling load and fundamental frequency of FG sandwich beams (C2-section, $\alpha_1 = \alpha_2 = \alpha_3 = 0.4$ and $p = 2$) with respect to L/b_3 for various BCs.

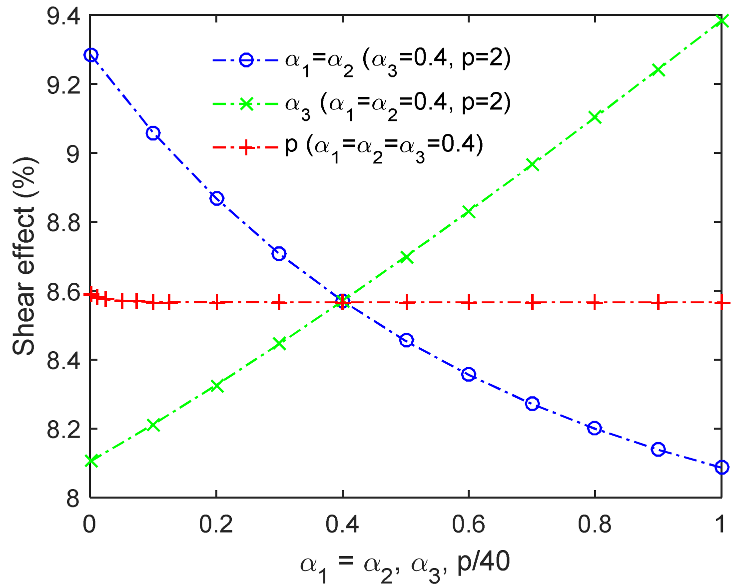

a. Critical buckling load

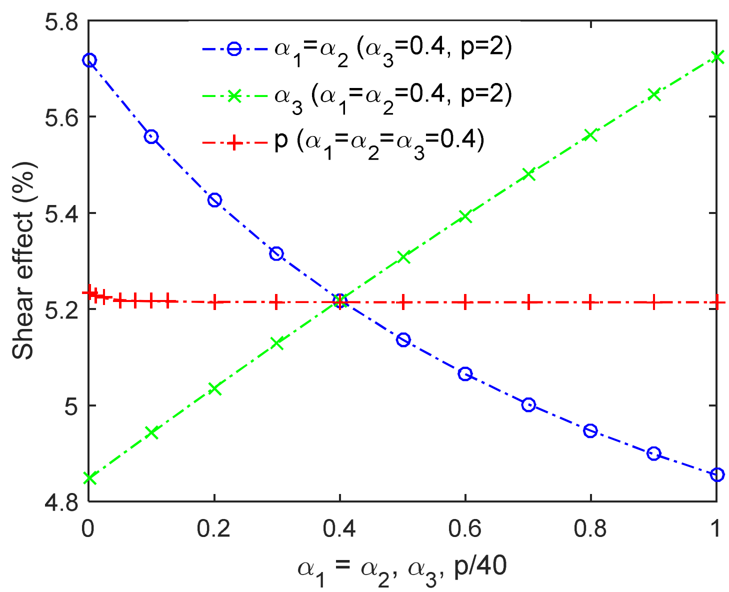

b. Fundamental frequency

Figure 10. Shear effect on the critical buckling load and fundamental frequency of FG sandwich C-C C2-beams ($L/b_3 = 5$) with respect to ceramic's thickness ratio or material parameter.

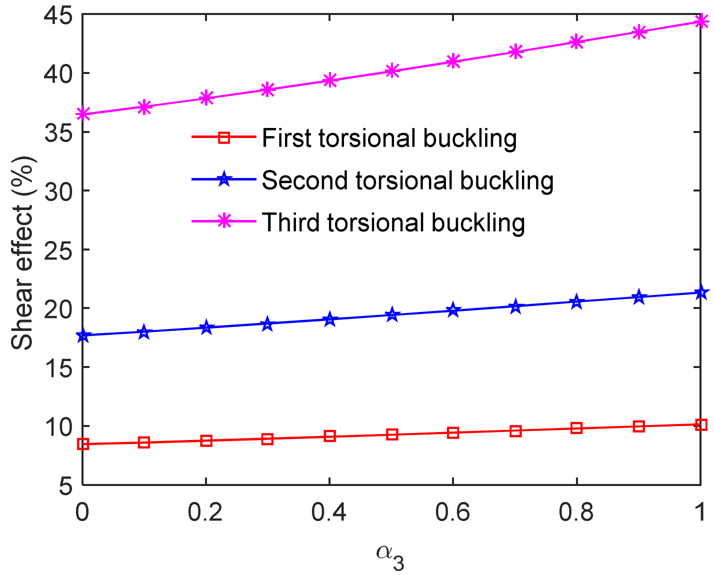

a. Buckling loads

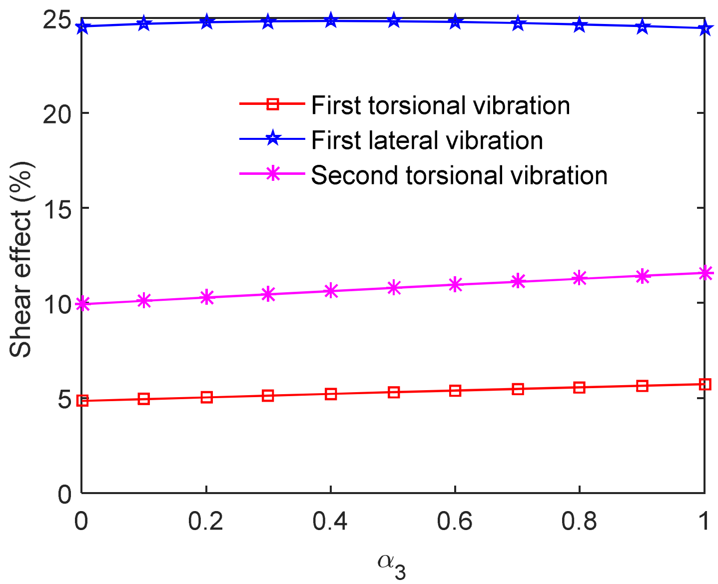

b. Natural frequency

Figure 11. Shear effect on first three buckling load and natural frequencies of FG sandwich C-C C2-beams ($\alpha_1 = \alpha_2 = 0.4$, $p = 2$ and $L / b_3 = 5$) with respect to ceramic's thickness ratio of web.

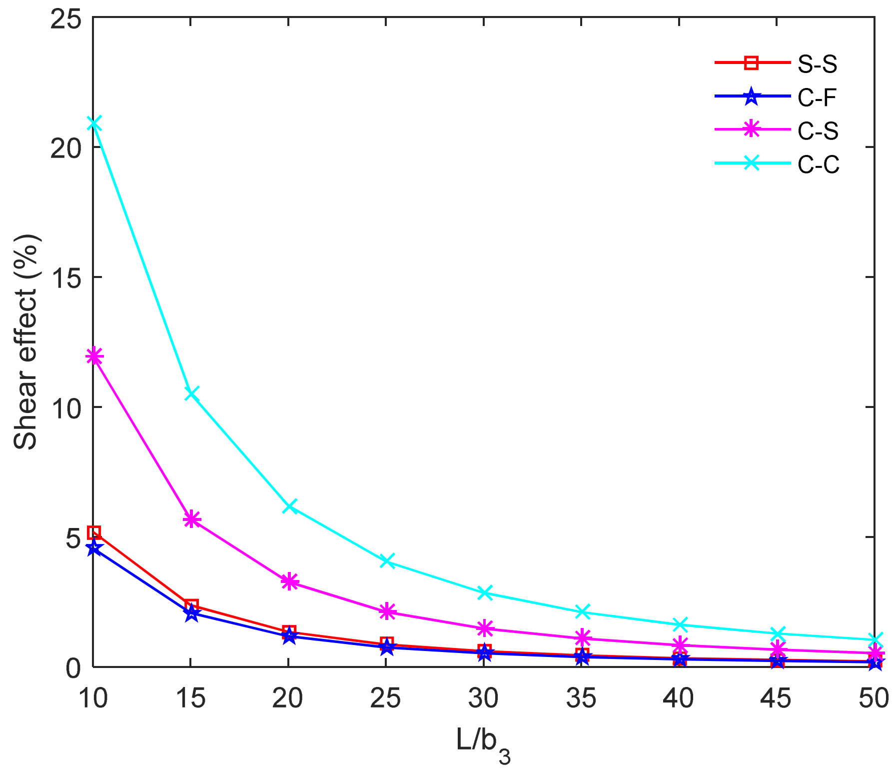

Figure 12. Shear effect on the deflections of composite C4-beams with $[45/-45]_{4S}$ in flanges and web with respect to L/b_3 for various BCs.

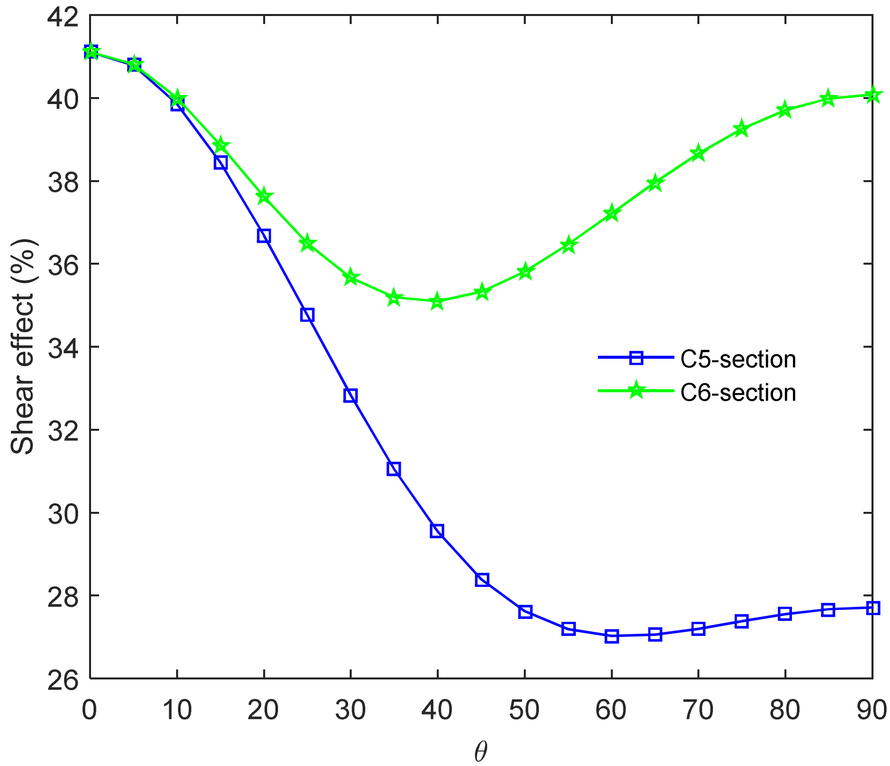

Figure 13. Shear effect on the deflections of composite C-C beams with C5- and C6- sections with respect to fiber orientation.

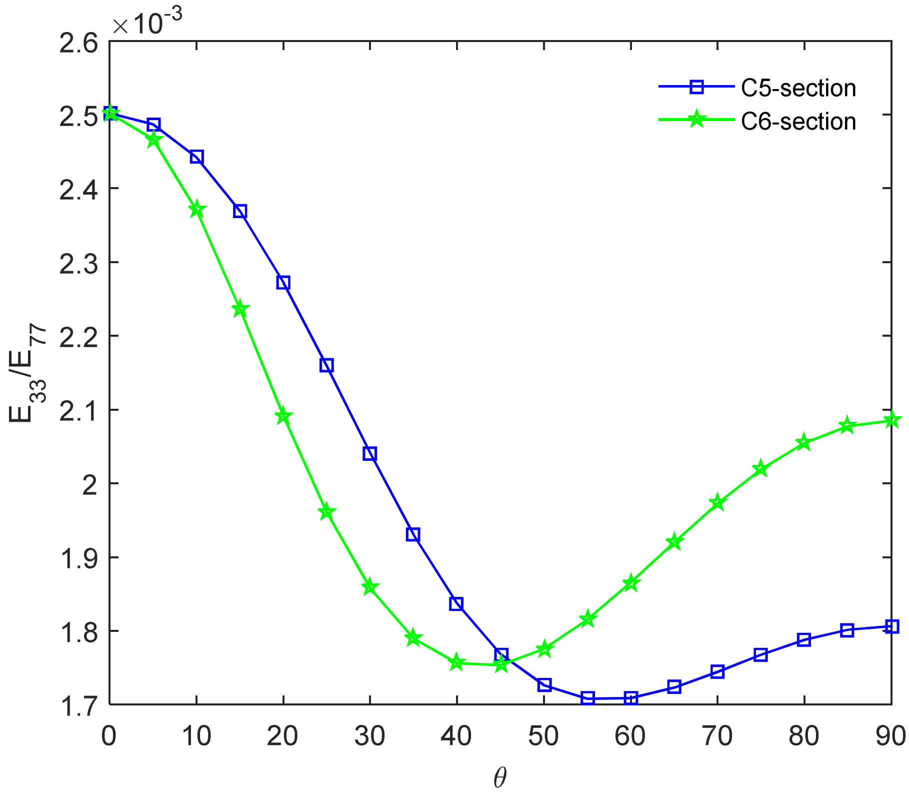

Figure 14 E_{33}/E_{77} ratio of composite channel beams for C5- and C6-section with respect to fiber orientation.

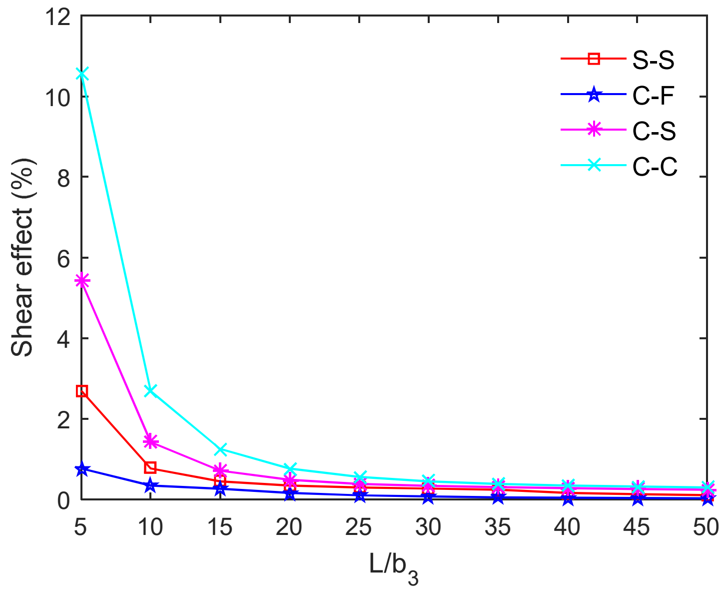

a. Critical buckling loads

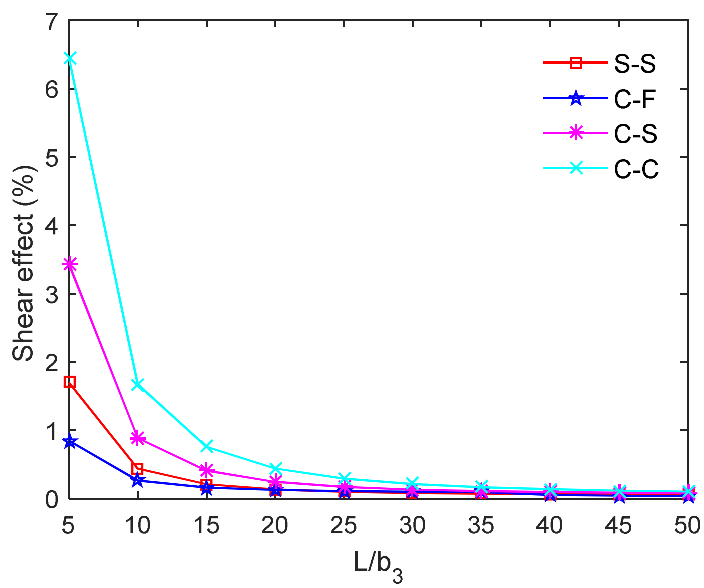

b. Fundamental frequency

Figure 15. Shear effect on the critical buckling load and fundamental frequency of composite C4-beams ($[45/-45]_{4S}$ in flanges and web) with respect to L/b_3 for various BCs.

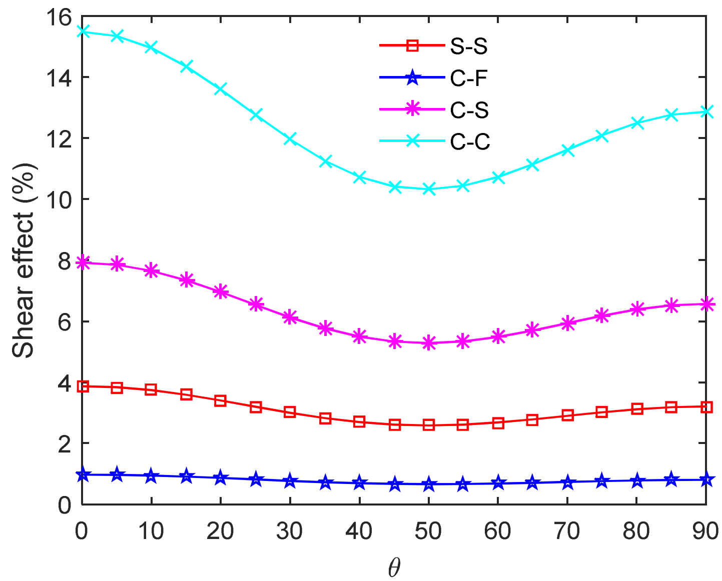

a. Fiber orientation in flanges ($[45/-45]_{4S}$ in web)

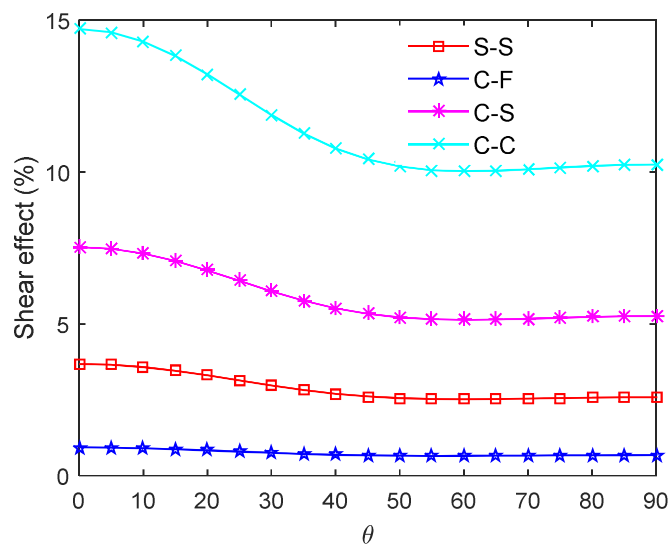

b. Fiber orientation in web ($[45/-45]_{4S}$ in flanges)

Figure 16. Shear effect on the critical buckling load of composite C4-beams ($L/b_3 = 5$) with respect to fiber orientation in flanges and web for various BCs.

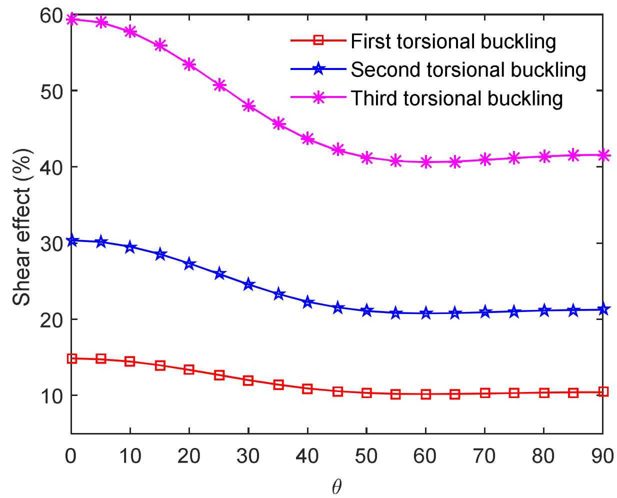

a. Buckling loads

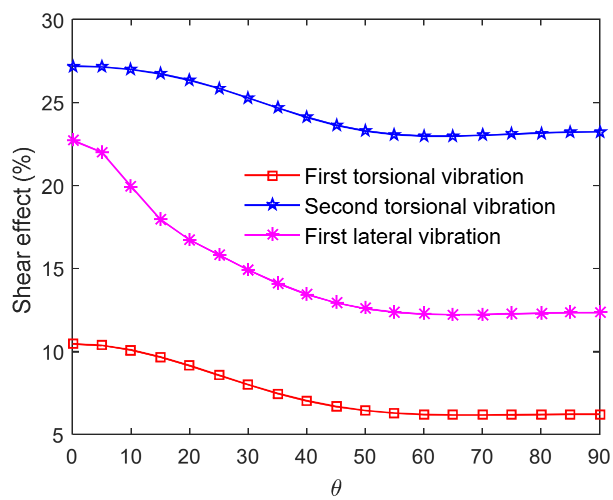

b. Natural frequencies

Figure 17. Shear effect on first three buckling loads and natural frequencies modes of composite C-C C4-beams ($[45/-45]_{4S}$ in flanges) with respect to fiber orientation in web.

Table 1. Shape functions and essential BCs of thin-walled channel beams.

BC	$\dfrac{\varphi_j(z)}{e^{\frac{-jz}{L}}}$	z=0	z=L
S-S	$\dfrac{z}{L}\left(1-\dfrac{z}{L}\right)$	$U=V=\phi=0$	$U=V=\phi=0$
C-F	$\left(\dfrac{z}{L}\right)^2$	$U=V=\phi=0$ $U'=V'=\phi'=0$ $W=\psi_y=\psi_x=\psi_\varpi=0$	
C-S	$\left(\dfrac{z}{L}\right)^2\left(1-\dfrac{z}{L}\right)$	$U=V=\phi=0$ $U'=V'=\phi'=0$ $W=\psi_y=\psi_x=\psi_\varpi=0$	$U=V=\phi=0$
C-C	$\left(\dfrac{z}{L}\right)^2\left(1-\dfrac{z}{L}\right)^2$	$U=V=\phi=0$ $U'=V'=\phi'=0$ $W=\psi_y=\psi_x=\psi_\varpi=0$	$U=V=\phi=0$ $U'=V'=\phi'=0$ $W=\psi_y=\psi_x=\psi_\varpi=0$

Table 2. Convergence studies of thin-walled FG sandwich channel beams.

BCs	Model	m=2	4	6	8	10	12	14
1. Mid-span deflections (mm)								
S-S	Shear	1.907	2.005	2.026	2.029	2.031	2.032	2.033
	No shear	1.875	1.971	1.990	1.993	1.994	1.995	1.996
C-F	Shear	3.876	4.032	4.060	4.063	4.066	4.067	4.068
	No shear	3.813	3.963	3.986	3.989	3.990	3.991	3.991
C-S	Shear	0.802	0.896	0.905	0.908	0.909	0.910	0.910
	No shear	0.770	0.863	0.869	0.872	0.872	0.873	0.873
C-C	Shear	0.519	0.527	0.532	0.534	0.534	0.536	0.536
	No shear	0.487	0.494	0.497	0.498	0.498	0.499	0.499
2. Critical buckling loads (kN)								
S-S	Shear	26.316	25.719	25.538	25.535	25.535	25.535	25.535
	No shear	26.346	25.751	25.570	25.568	25.568	25.568	25.568
C-F	Shear	6.756	6.392	6.392	6.392	6.392	6.392	6.392
	No shear	6.759	6.395	6.395	6.395	6.395	6.395	6.395
C-S	Shear	45.352	42.303	42.245	42.245	42.245	42.245	42.245
	No shear	45.597	42.539	42.481	42.481	42.481	42.481	42.481
C-C	Shear	72.139	71.474	71.357	71.357	71.357	71.357	71.357
	No shear	72.510	71.841	71.723	71.723	71.723	71.723	71.723
3. The fundamental frequencies (Hz)								
S-S	Shear	18.880	18.633	18.564	18.563	18.563	18.563	18.563
	No shear	18.896	18.650	18.580	18.579	18.579	18.579	18.579
C-F	Shear	6.713	6.623	6.618	6.617	6.617	6.617	6.617
	No shear	6.716	6.626	6.621	6.621	6.621	6.621	6.621
C-S	Shear	26.889	26.333	26.324	26.324	26.324	26.324	26.324
	No shear	27.115	26.567	26.559	26.559	26.559	26.559	26.559
C-C	Shear	35.550	35.383	35.379	35.377	35.376	35.376	35.376
	No shear	35.768	35.605	35.604	35.604	35.604	35.604	35.604

Table 3. Convergence studies of thin-walled composite channel beams.

BCs	Model	m=2	4	6	8	10	12	14
1. Mid-span deflections (mm)								
S-S	Shear	6.385	6.715	6.786	6.796	6.803	6.807	6.810
	No shear	6.256	6.575	6.641	6.650	6.655	6.657	6.658
C-F	Shear	12.977	13.500	13.598	13.607	13.619	13.623	13.626
	No shear	12.722	13.223	13.300	13.309	13.315	13.317	13.318
C-S	Shear	2.699	3.013	3.045	3.056	3.060	3.063	3.064
	No shear	2.568	2.879	2.901	2.909	2.911	2.912	2.912
C-C	Shear	1.753	1.783	1.799	1.807	1.809	1.814	1.814
	No shear	1.625	1.649	1.657	1.660	1.662	1.663	1.664
2. Critical buckling loads (kN)								
S-S	Shear	4.972	4.859	4.825	4.825	4.825	4.825	4.825
	No shear	4.984	4.870	4.836	4.835	4.835	4.835	4.835
C-F	Shear	1.277	1.208	1.208	1.208	1.208	1.208	1.208
	No shear	1.278	1.209	1.209	1.209	1.209	1.209	1.209
C-S	Shear	10.841	9.865	9.847	9.847	9.847	9.847	9.847
	No shear	10.896	9.910	9.892	9.892	9.892	9.892	9.892
C-C	Shear	16.295	16.170	16.148	16.148	16.148	16.148	16.148
	No shear	16.389	16.263	16.240	16.240	16.240	16.240	16.240
3. The fundamental frequencies (Hz)								
S-S	Shear	55.180	54.459	54.255	54.252	54.252	54.252	54.252
	No shear	55.262	54.538	54.333	54.330	54.330	54.330	54.330
C-F	Shear	19.621	19.358	19.343	19.342	19.342	19.341	19.341
	No shear	19.634	19.371	19.356	19.355	19.355	19.355	19.355
C-S	Shear	87.520	84.667	84.623	84.622	84.621	84.621	84.621
	No shear	87.786	84.916	84.874	84.874	84.874	84.874	84.874
C-C	Shear	112.686	111.973	111.945	111.934	111.929	111.927	111.926
	No shear	113.047	112.374	112.365	112.365	112.365	112.365	112.365

Table 4. Comparison of the critical buckling load of C1-beams (*kN*)

BCs	Reference	p =0	0.5	1	2	5	10
S-S	Present (Shear)	776.278	594.574	509.456	429.022	350.578	312.060
	Present (No shear)	778.265	597.312	513.747	434.010	353.787	313.688
	Lanc et al. (2016) (No shear)	780.153	601.903	518.922	438.979	357.429	316.213
C-F	Present (Shear)	263.747	203.379	173.556	144.095	115.143	102.208
	Present (No shear)	264.029	203.579	173.714	144.223	115.253	102.311
	Lanc et al. (2016) (No shear)	264.038	203.605	173.752	144.258	115.272	102.321
C-S	Present (Shear)	1414.959	1088.613	931.698	779.988	630.954	560.598
	Present (No shear)	1422.236	1094.418	938.226	786.652	635.630	563.744
	Lanc et al. (2016) (No shear)	1427.730	1105.210	950.041	797.849	643.889	569.606
C-C	Present (Shear)	2598.438	2004.193	1714.215	1430.336	1150.364	1020.995
	Present (No shear)	2624.444	2022.495	1730.650	1444.845	1161.556	1030.365
	Lanc et al. (2016) (No shear)	2648.370	2053.970	1762.670	1474.170	1183.630	1047.040

Table 5. Comparison of the first four non-dimensional frequencies of S-S beams with C1-section.

Reference	Frequency	p=0	0.5	1	2	5	10
Present (Shear)	$\bar{\omega}_1$	3.0659	2.7541	2.5544	2.3114	2.0048	1.8349
	$\bar{\omega}_2$	4.3462	3.8270	3.5533	3.2895	3.0075	2.8059
	$\bar{\omega}_3$	10.1965	9.1416	8.4879	7.7173	6.7663	6.2169
	$\bar{\omega}_4$	12.0939	10.7356	9.9661	9.1447	8.0110	7.3327
Present (No shear)	$\bar{\omega}_1$	3.0668	2.7549	2.5551	2.3119	2.0054	1.8354
	$\bar{\omega}_2$	4.3475	3.8653	3.6402	3.4168	3.1088	2.8599
	$\bar{\omega}_3$	10.2254	9.2126	8.5910	7.8480	6.8848	6.2971
	$\bar{\omega}_4$	12.1028	10.7996	10.1011	9.2302	8.0168	7.3391
Nguyen, Kim and Lee (2016b) (No shear)	$\bar{\omega}_1$	3.0668	2.7612	2.5642	2.3227	2.0148	1.8421
	$\bar{\omega}_2$	4.3475	3.8641	3.6385	3.4141	3.1054	2.8575
	$\bar{\omega}_3$	10.2254	9.2060	8.5828	7.8407	6.8811	6.2951
	$\bar{\omega}_4$	12.1029	10.8223	10.1441	9.2903	8.0589	7.3684

Table 6. Mid-span deflections at of thin-walled FG channel C1-beams subject to a uniform load (q_y = 0.5 *kN*/*m*) (*mm*).

L/b_3	BC	Model	*p*					
			0	0.5	1	2	5	10
20	S-S	Present (Shear)	0.396	0.510	0.596	0.716	0.897	1.014
		Present (No shear)	0.390	0.502	0.586	0.705	0.883	0.998
	C-F	Present (Shear)	1.343	1.730	2.021	2.429	3.044	3.440
		Present (No shear)	1.325	1.706	1.993	2.396	3.003	3.393
	C-S	Present (Shear)	0.162	0.209	0.244	0.293	0.367	0.415
		Present (No shear)	0.156	0.201	0.235	0.282	0.353	0.399
	C-C	Present (Shear)	0.084	0.108	0.126	0.152	0.190	0.215
		Present (No shear)	0.078	0.100	0.117	0.141	0.177	0.200
50	S-S	Present (Shear)	15.261	19.654	22.958	27.596	34.583	39.080
		Present (No shear)	15.223	19.605	22.900	27.527	34.496	38.982
	C-F	Present (Shear)	51.872	66.802	78.030	93.796	117.543	132.829
		Present (No shear)	51.759	66.655	77.859	93.590	117.285	132.539
	C-S	Present (Shear)	6.127	7.891	9.217	11.080	13.885	15.690
		Present (No shear)	6.089	7.842	9.160	11.011	13.798	15.593
	C-C	Present (Shear)	3.082	3.969	4.637	5.573	6.984	7.893
		Present (No shear)	3.045	3.921	4.580	5.505	6.899	7.797

Table 7. Mid-span deflections of thin-walled FG channel C2-beams subject to a uniform load ($\alpha_1 = \alpha_2 = \alpha_3 = 0.4$, $q_y = 0.5$ *kN/m*) (*mm*).

L/b_3	BC	Model	*p*					
			0	0.5	1	2	5	10
20	S-S	Present (Shear)	0.396	0.457	0.496	0.541	0.595	0.624
		Present (No shear)	0.390	0.450	0.488	0.533	0.586	0.614
	C-F	Present (Shear)	1.343	1.551	1.681	1.835	2.021	2.118
		Present (No shear)	1.325	1.530	1.659	1.811	1.993	2.089
	C-S	Present (Shear)	0.162	0.187	0.203	0.221	0.244	0.255
		Present (No shear)	0.156	0.180	0.195	0.213	0.235	0.246
	C-C	Present (Shear)	0.084	0.097	0.105	0.115	0.126	0.132
		Present (No shear)	0.078	0.090	0.098	0.107	0.117	0.123
50	S-S	Present (Shear)	15.261	17.625	19.104	20.855	22.958	24.061
		Present (No shear)	15.223	17.581	19.057	20.803	22.901	24.001
	C-F	Present (Shear)	51.872	59.906	64.934	70.884	78.033	81.782
		Present (No shear)	51.759	59.775	64.792	70.729	77.863	81.604
	C-S	Present (Shear)	6.127	7.076	7.670	8.373	9.218	9.660
		Present (No shear)	6.089	7.032	7.623	8.321	9.160	9.600
	C-C	Present (Shear)	3.082	3.560	3.858	4.212	4.637	4.859
		Present (No shear)	3.045	3.516	3.811	4.161	4.580	4.800

Table 8. Mid-span deflections of thin-walled FG channel C3-beams subject to a uniform load ($\alpha_1 = \alpha_2 = 0.9$ and $\alpha_3 = 0.1$, $q_y = 0.5$ *kN/m*) (*mm*).

L/b_3	BC	Model	p					
			0	0.5	1	2	5	10
20	S-S	Present (Shear)	0.396	0.425	0.441	0.459	0.478	0.487
		Present (No shear)	0.390	0.418	0.433	0.450	0.468	0.477
	C-F	Present (Shear)	1.343	1.441	1.496	1.555	1.619	1.650
		Present (No shear)	1.325	1.420	1.473	1.530	1.592	1.622
	C-S	Present (Shear)	0.162	0.174	0.181	0.188	0.197	0.200
		Present (No shear)	0.156	0.167	0.173	0.180	0.187	0.191
	C-C	Present (Shear)	0.084	0.091	0.094	0.098	0.103	0.105
		Present (No shear)	0.078	0.084	0.087	0.090	0.094	0.095
50	S-S	Present (Shear)	15.261	16.361	16.974	17.633	18.347	18.690
		Present (No shear)	15.223	16.317	16.925	17.581	18.289	18.629
	C-F	Present (Shear)	51.872	55.610	57.689	59.930	62.353	63.520
		Present (No shear)	51.759	55.478	57.546	59.774	62.181	63.340
	C-S	Present (Shear)	6.127	6.571	6.818	7.085	7.373	7.512
		Present (No shear)	6.089	5.627	6.770	7.032	7.315	7.452
	C-C	Present (Shear)	3.082	3.307	3.432	3.568	3.715	3.786
		Present (No shear)	3.045	3.263	3.385	3.516	3.658	3.726

Table 9. Comparison of the maximum deflections of thin-walled composite channel C-F beams subjected to a vertical concentrated load $(P_y = 1kN)$ at end free (*mm*).

Reference	Lay-up						
	$[0]_{16}$	$\begin{bmatrix}15/\\-15\end{bmatrix}_{4s}$	$\begin{bmatrix}30/\\-30\end{bmatrix}_{4s}$	$\begin{bmatrix}45/\\-45\end{bmatrix}_{4s}$	$\begin{bmatrix}60/\\-60\end{bmatrix}_{4s}$	$\begin{bmatrix}75/\\-75\end{bmatrix}_{4s}$	$\begin{bmatrix}0/\\90\end{bmatrix}_{4s}$
Present (Shear)	72.291	79.845	107.188	154.586	195.326	212.101	108.109
Kim, Jeon and Lee (2013) (Shear)	72.627	80.075	107.270	154.570	195.260	212.120	107.790
Present (No shear)	71.486	79.122	106.556	153.929	194.544	211.170	107.219
Kim, Jeon and Lee (2013) (No shear)	71.399	79.211	106.150	154.220	193.410	211.160	106.530

Table 10. Comparison of the critical buckling load of thin-walled composite channel C-F beams (kN).

Lay-up	Reference	
	Present (Shear)	Kim and Lee (2014) (Shear)
$[0]_{16}$	0.9858	0.9858
$[15/-15]_{4s}$	0.8907	0.8907
$[30/-30]_{4s}$	0.6615	0.6615
$[45/-45]_{4s}$	0.4579	0.4580
$[60/-60]_{4s}$	0.3623	0.3624
$[75/-75]_{4s}$	0.3338	0.3338
$[90/-90]_{4s}$	0.3287	0.3287

Table 11. Comparison of the fundamental frequencies of thin-walled composite channel C-F beams (Hz).

Lay-up	Reference			
	Present (Shear)	Kim and Lee (2014) (Shear)	Present (No Shear)	Kim and Lee (2014) (No Shear)
$[0]_{16}$	18.418	18.40	18.430	18.43
$[15/-15]_{4s}$	17.508	17.50	17.518	17.52
$[30/-30]_{4s}$	15.089	15.09	15.095	15.09
$[45/-45]_{4s}$	12.555	12.55	12.559	12.56
$[60/-60]_{4s}$	11.168	11.17	11.172	11.17
$[75/-75]_{4s}$	10.719	10.72	10.723	10.72
$[90/-90]_{4s}$	10.637	10.64	10.641	10.64

Table 12. Mid-span deflections of thin-walled composite beams with C4-section subjected to a uniform load ($q_y = 0.1kN/m$) (mm).

L/b_3	BC	Model	Lay-up						
			$[0]_{16}$	$\begin{bmatrix}15/\\-15\end{bmatrix}_{4s}$	$\begin{bmatrix}30/\\-30\end{bmatrix}_{4s}$	$\begin{bmatrix}45/\\-45\end{bmatrix}_{4s}$	$\begin{bmatrix}60/\\-60\end{bmatrix}_{4s}$	$\begin{bmatrix}75/\\-75\end{bmatrix}_{4s}$	$\begin{bmatrix}0/\\90\end{bmatrix}_{4s}$
20	S-S	Present (Shear)	0.289	0.318	0.424	0.610	0.770	0.837	0.430
		Present (No shear)	0.279	0.309	0.416	0.601	0.760	0.825	0.419
	C-F	Present (Shear)	0.979	1.078	1.439	2.069	2.613	2.839	1.457
		Present (No shear)	0.949	1.051	1.415	2.044	2.584	2.805	1.424
	C-S	Present (Shear)	0.122	0.133	0.174	0.249	0.314	0.342	0.179
		Present (No shear)	0.112	0.124	0.167	0.241	0.304	0.330	0.168
	C-C	Present (Shear)	0.066	0.071	0.091	0.128	0.162	0.177	0.095
		Present (No shear)	0.056	0.062	0.083	0.120	0.152	0.165	0.084
50	S-S	Present (Shear)	10.971	12.130	16.309	23.539	29.746	32.295	16.430
		Present (No shear)	10.908	12.073	16.259	23.488	29.685	32.222	16.360
	C-F	Present (Shear)	37.274	41.217	55.428	80.011	101.111	109.771	55.832
		Present (No shear)	37.087	41.049	55.281	79.858	100.929	109.555	55.625
	C-S	Present (Shear)	4.426	4.886	6.553	9.446	11.935	12.962	6.614
		Present (No shear)	4.363	4.829	6.504	9.395	11.874	12.889	6.544
	C-C	Present (Shear)	2.244	2.470	3.300	4.748	5.997	6.516	3.341
		Present (No shear)	2.182	2.415	3.252	4.698	5.937	6.444	3.272